

14 July 2015

To: CSET data-processing file
FROM: Al Cooper
SUBJECT: Data review: Using the 'Review.R' program

1 General description

This is an update of the general description, adapted for CSET and using CSET research flight 3 as an example for discussion of the plots. This program (~cooperw/RStudio/CSET/Review.R, also available at this github URL) uses a set of functions to make plots that are designed to provide a starting point for quality assessment. This structure makes it easy to change the set of plots for a particular project, to refine the time range for plots, to re-generate a subset of the plots, to add new plots, and otherwise to tailor the output to project and personal needs. This memo shows typical output from the program, suggests how each plot should look and how to spot problems, and provides a record of how output should look when systems are functioning properly.

The program can be used in different ways. The simplest is to source("Review.R") from an R console, including the console in RStudio. The program asks for a project and flight, uses a standard set of plots or allows a user to change that set interactively, and then produces a PDF file that is a concatenation of the plots produced. PNG files could also be produced and would provide a much smaller output size, but PDFs have the advantage of maintaining quality when magnified (and are also easier to concatenate) so that has been selected even though that format produces large files (of typical size 10 MB).

Other ways to use the Review.R script and routines include:

1. After running the script, the individual plot functions are available and the assignment of plots to the PDF file has been cancelled, so you can re-generate any selected plots for console or RStudio display, optionally with variable or time-segment modifications.
2. 'Review.R' can be incorporated into an Rnw document where comments can be added to provide a record of problems identified or needing further study, and this might be useful documentation to preserve and distribute. This document is an example of that use.
3. It may be useful to make the plot functions in this routine available as a package so they can be used easily without needing the full structure of 'Review.R'

```
## [1] "Project is CSET"
## [1] "Flight is rf03"
```

2 Running the program

When the program is run as an R script, it will interactively ask for a flight name, and description of the plots desired. The flight name should have the format “rf09” (without quote marks). The plot description can be 0 (all plots), -1 (project default set), or a series of plots in the format “c(3,5,7)” (without quotes). A CR reply selects the default set of plots for the project.

3 Interpreting the plots

These are short descriptions of the plots generated by each plot function:

- RPlot1: construct flight track with map and height-vs-time
- RPlot2: construct one-per-hour track plots (omitted from default)
- RPlot3: all temperatures, one plot
- RPlot4: scatterplots and differences, individual pairs of temperatures
- RPlot5: all humidity
 - “ “ scatterplots, humidity measurements
 - “ “ dew point cavity pressures; VCSEL laser intensity
 - “ “ vapor pressure, mixing ratio, relative humidity
- RPlot6: ambient pressures
- RPlot7: dynamic pressures
 - “ “ TAS and MACH
- RPlot8: total pressure (static + dynamic)
- RPlot9: wind components
 - “ “ horizontal wind, E and N components
- RPlot10: ground speed components (Schuler oscillation) and GGQUAL
- RPlot11: attack, sideslip
- RPlot12: IRU attitude-angle comparisons
- RPlot13: IRU continued, ACINS, VSPD, altitude
- RPlot14: not present now
- RPlot15: Concentrations: CN, CDP, UHSAS
 - “ “ QC housekeeping: flows, laser intensity, CN/UHSAS
- RPlot16: mean diameters
 - “ “ liquid water content
 - “ “ CDP housekeeping
- RPlot17: all-flight Skew-T
- RPlot18: plot skew-T for individual climbs and descents: (omitted from default)
- RPlot19: potential-temperature history plots
 - “ “ vertical-profile potential temperature plots
- RPlot20: CDP sample size distributions
- RPlot21: radiometric measurements (surface T and IR irradiance)

RPlot22:UHSAS sample size distributions

RPlot30: CO and O3

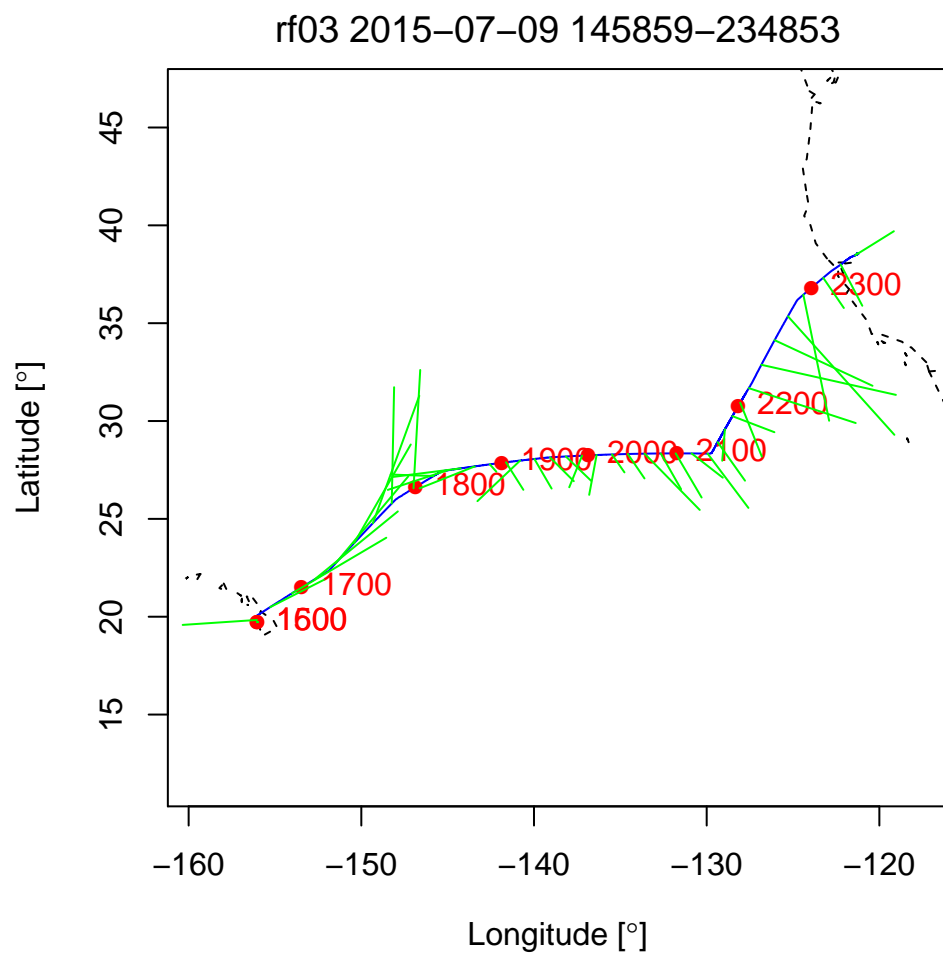
“ “ CO inlet pressure

These names correspond to the names of functions, not necessarily to the plot numbers, because many of the functions generate several plots and it is also possible to generate only a subset of the plots. In the following description of the plots, proper figure numbers for the project-default selections are used for this example, but the numbering may change. The sequence, however, should remain the same.

The plots in this memo are reduced in size compared to the PDF file that is generated by running Review.R. When using this guide, it may be useful to refer to the full-scale plots because some of the legends and other features are hard to read at this reduced size. For each plot, a few-paragraph description is provided. The intent of those descriptions is to suggest how to interpret the plot as an indicator of potential problems. Therefore, most of the descriptions give expected tolerances for differences among sensors or other quantifiable departures from expected behavior that should trigger further investigation of the measurements. That is the intent of these plots: To provide quick indications of problems so that they can be investigated further, usually with other tools. Users should pay particular attention to the tolerances denoted on many plots by dashed lines and to the titles where mean differences between redundant measurements are listed. Once a “good” set of plots is obtained for a project, that set should be used as a reference for future flights because changes in the patterns, even more than tests against specified tolerances, are the best indicators of problems.

Flight track: The first plot function generates two flight-track plots, Fig. 1 a plan-view and Fig. 2 showing height-vs-time. These provide general context that may be useful when looking at the remaining plots, but they can be suppressed if desired because they usually don’t indicate problems with data quality. In some cases the flight track becomes overlaid to such an extent that it is hard to use, so for such cases it may be useful to enable nplot=2, which plots separate flight tracks for each hour of flight. Normally this is disabled as not particularly useful for quality-review of the data.

Air temperature: Figure 3 shows the time history of measured air temperature from the various temperature sensors, and Fig. 4 compares these sensors in pairs of measurements. After all corrections, these should agree to within about 1°C; claimed uncertainty is about 0.3°C. ATH1, ATH2 and ATF1 should agree to within about 0.3°C. AT_A, the temperature from the aircraft avionics system, will often show larger scatter; this should not be considered a problem unless it exceeds about 2 C. It appears mostly because that measurement has slow response, either from filtering or delays or both, and this usually accounts for the errors. Differences in response times also leads to differences between ATF1 and ATH2 during climbs and descents, as is evident on the right side of the plot in the lower left panel. It is common to see two lines on the AT_A-vs-ATH2 or ATF1-vs-ATH2 plot for the same reason; one is from measurements during climb and the other from those



CSET RF03 2015-07-09 14:58:59–23:48:53 UTC, generated by RPlot1 2015-07-14 07:46:16 MD1

Figure 1: Flight track for CSET flight rf03 on 2015-07-09, 145859–234853 UTC

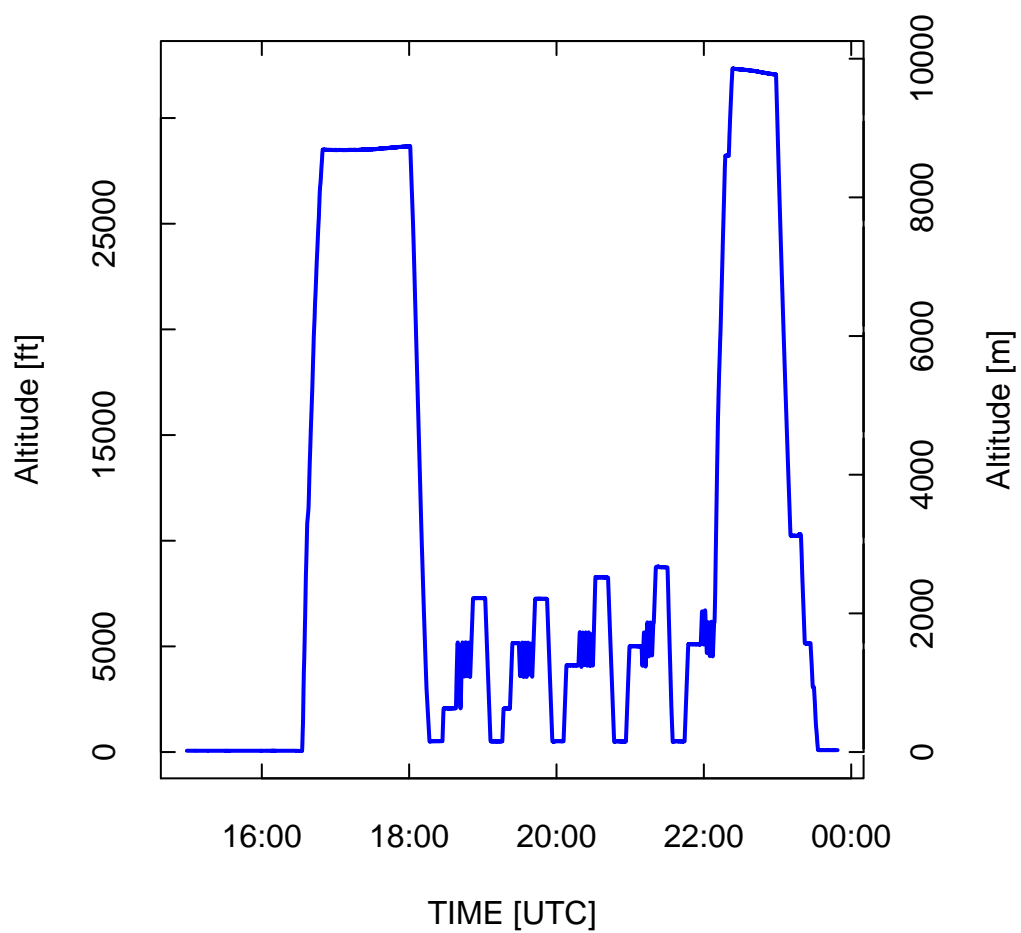
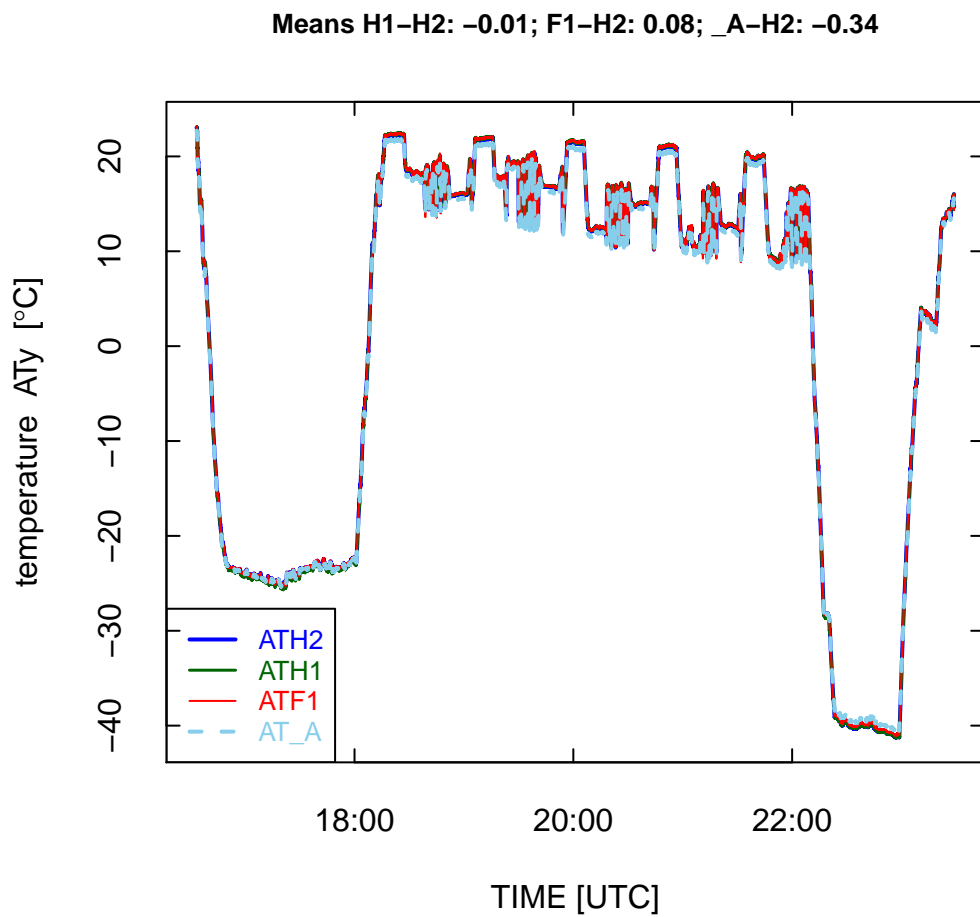
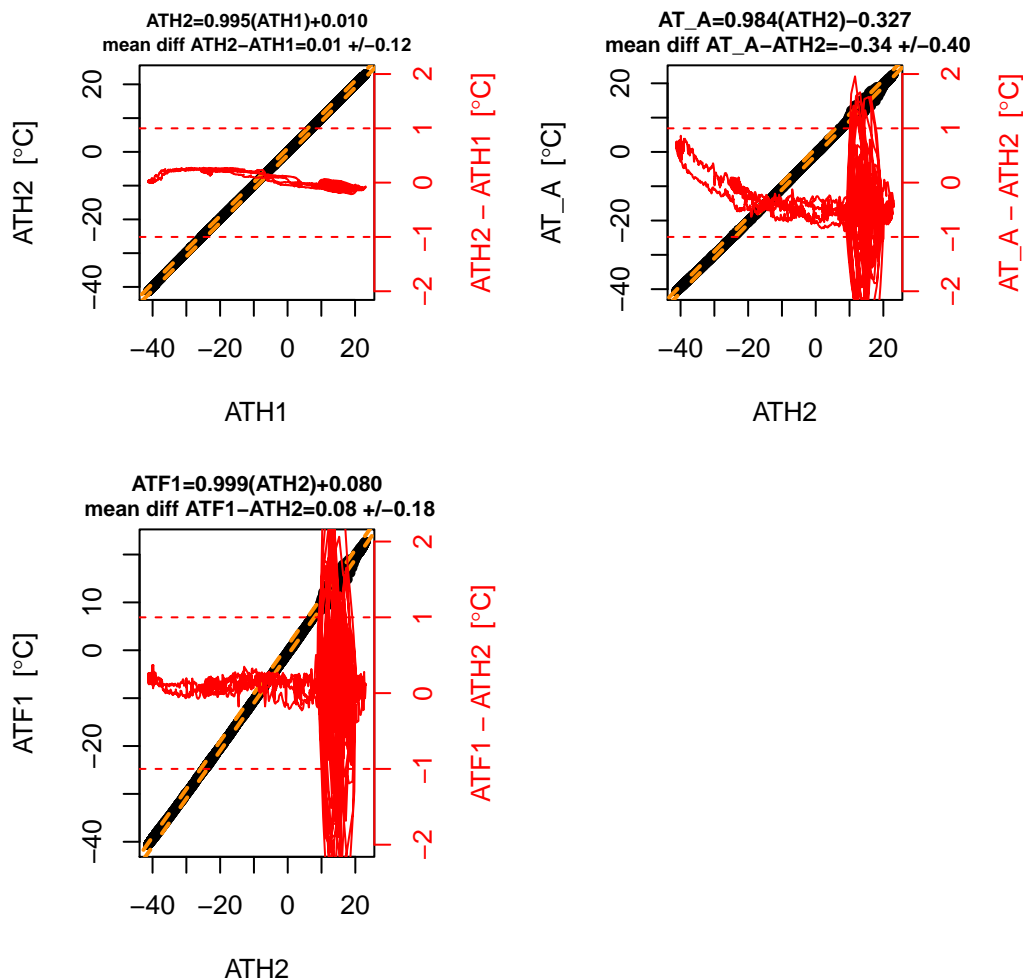


Figure 2: Height vs. time for CSET flight rf03 on 2015-07-09, 145859–234853 UTC



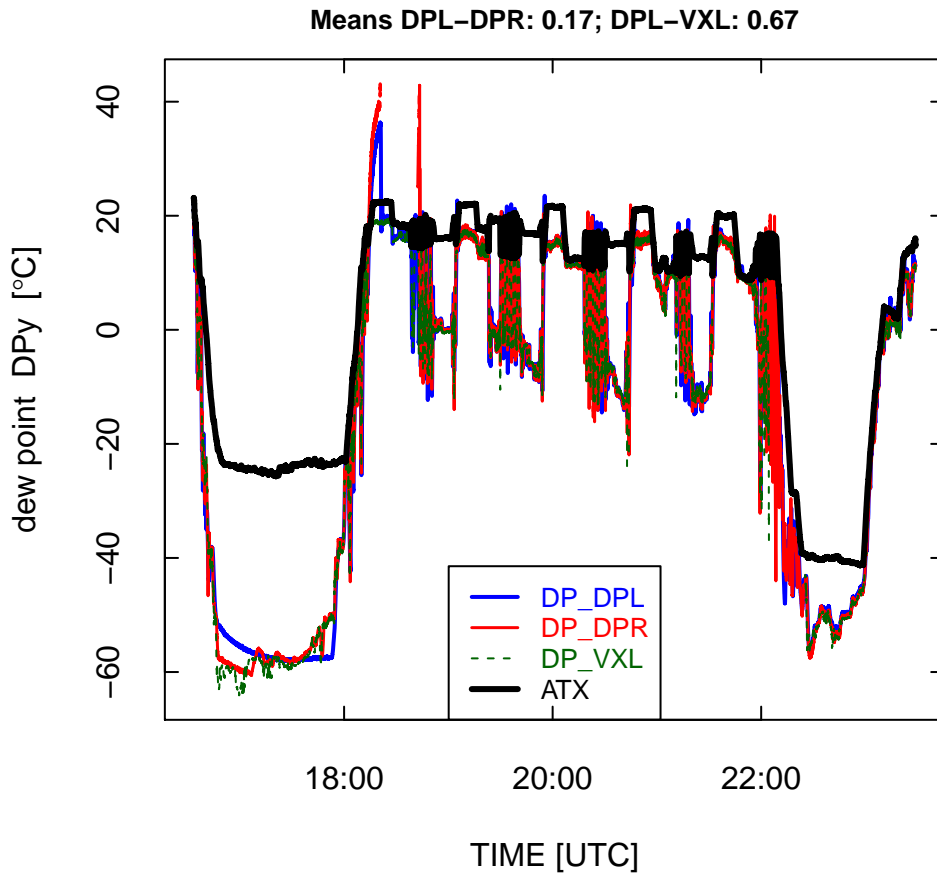
CSET RF03 2015-07-09 14:58:59–23:48:53 UTC, generated by RPlot3 2015-07-14 07:46:16 MD1

Figure 3: Air temperature (ATy) determined from the different temperature sensors.



CSET RF03 2015-07-09 14:58:59–23:48:53 UTC, generated by RPlot4 2015-07-14 07:46:16 MD1

Figure 4: Air temperature (ATy) determined from the different temperature sensors.



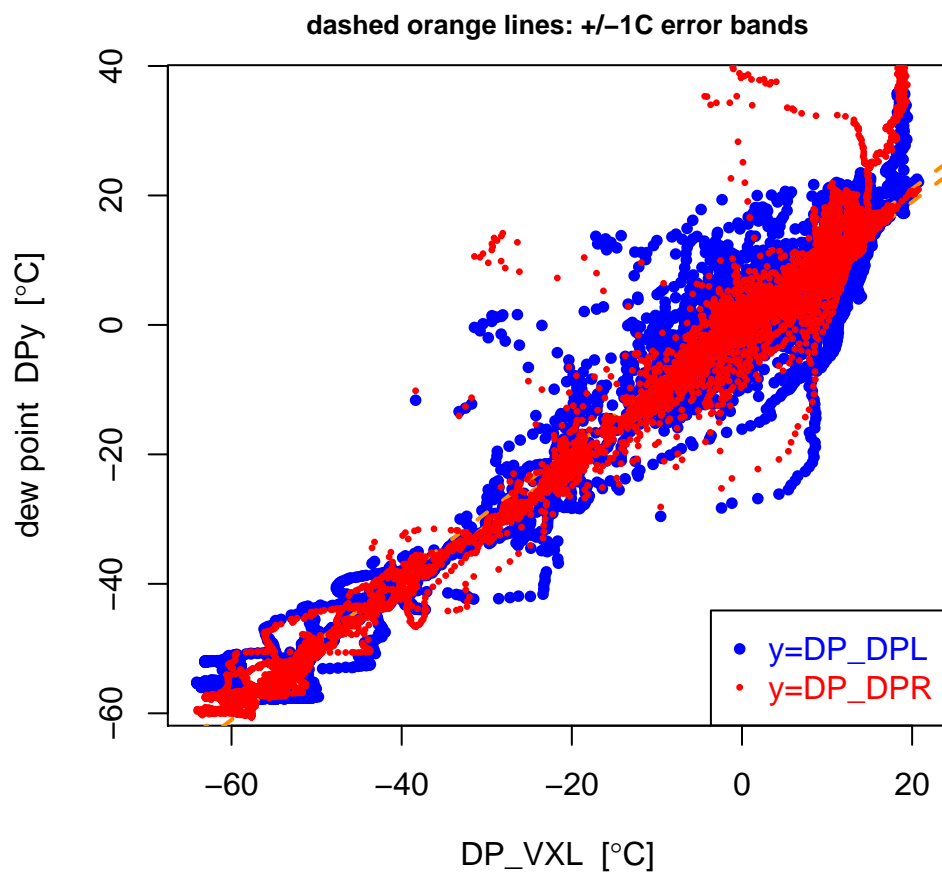
CSET RF03 2015–07–09 14:58:59–23:48:53 UTC, generated by RPlot5 2015–07–14 07:46:16 MD1

Figure 5: History of measurements of dew point from the available measurements.

during descent. For this flight, AT_A is higher than ATH1 or ATH2 when the temperature is lower than about -20°C; this has been common in CSET flights.

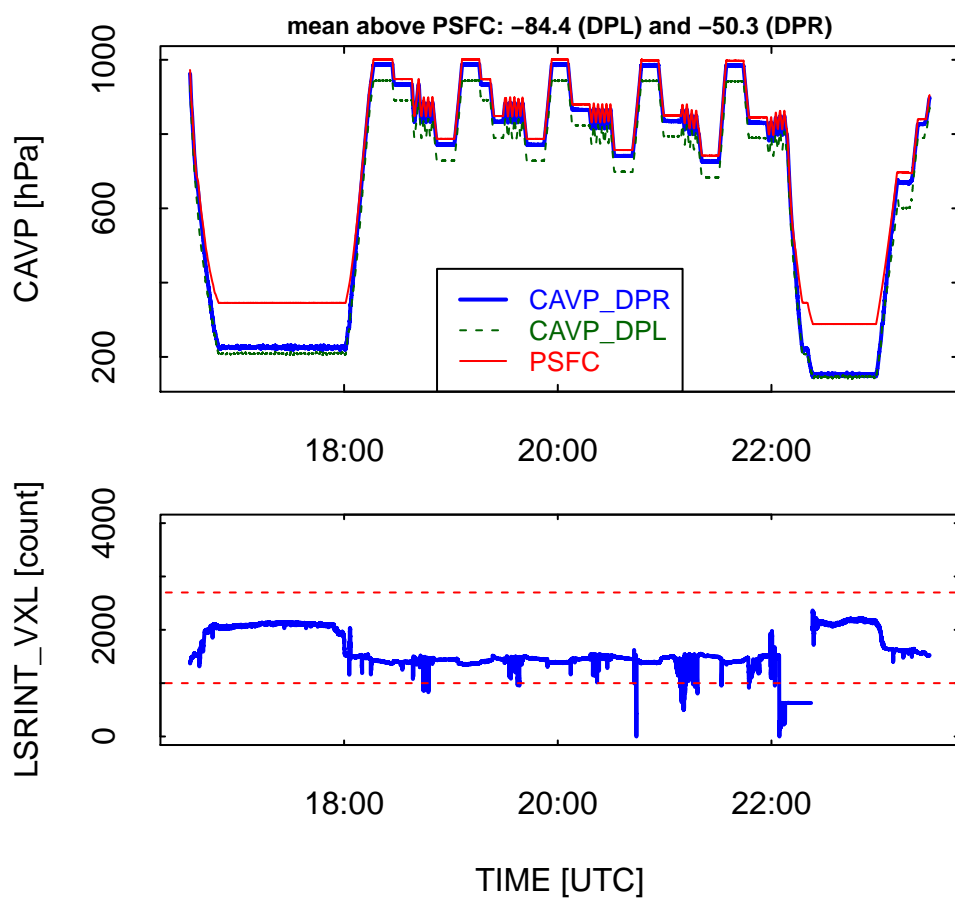
Humidity: Four plots are generated by function RPlot5). The first (Fig. 5) shows the history of various measurements of dew point, including those from the VCSEL for which dew point must be calculated from the direct measurements.

Agreement among these measurements to within about 1°C is good. It is common to have problems during and after descent, like that shown near 18:15 on this plot, where the dew-point sensors overheat in an effort to remove thick condensate that forms when the temperature increases rapidly. ATX is also plotted on this history to provide a reference: When the dew point temperature exceeds the temperature, even by a few degrees, there is very likely a problem because this almost never occurs in reality. DP_DPL has been responding more slowly than has DP_DPR; the latter is matching the VCSEL measurements fairly well except at points of overshoot following descents.



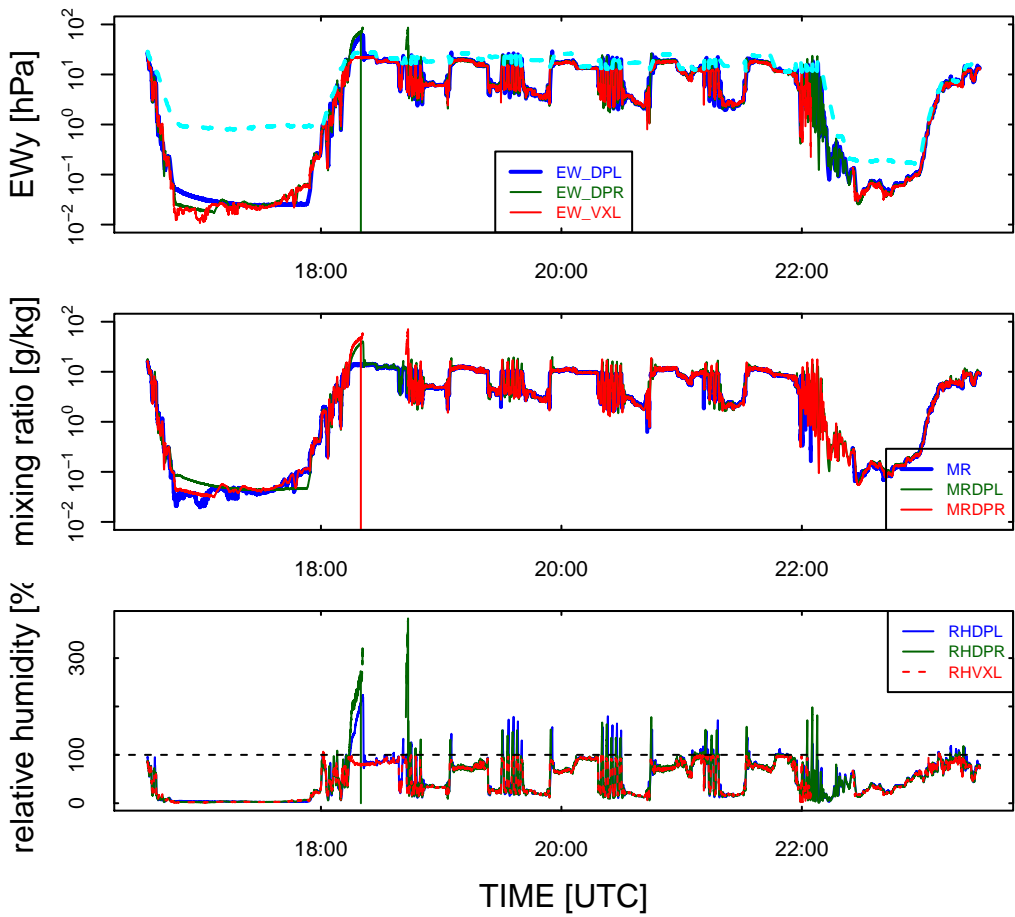
CSET RF03 2015-07-09 14:58:59-23:48:53 UTC, generated by RPlot5 2015-07-14 07:46:16 MD1

Figure 6: Comparison of available measurements to DP_DPB as a reference.



CSET RF03 2015-07-09 14:58:59-23:48:53 UTC, generated by RPlot5 2015-07-14 07:46:16 MD1

Figure 7: Pressures in the cavities of the dew-point sensors, plotted with the ambient pressure (PSXC) for reference.



CSET RF03 2015-07-09 14:58:59-23:48:53 UTC, generated by RPlot5 2015-07-14 07:46:16 MD1

Figure 8: Measurements of water vapor pressure, mixing ratio and relative humidity.

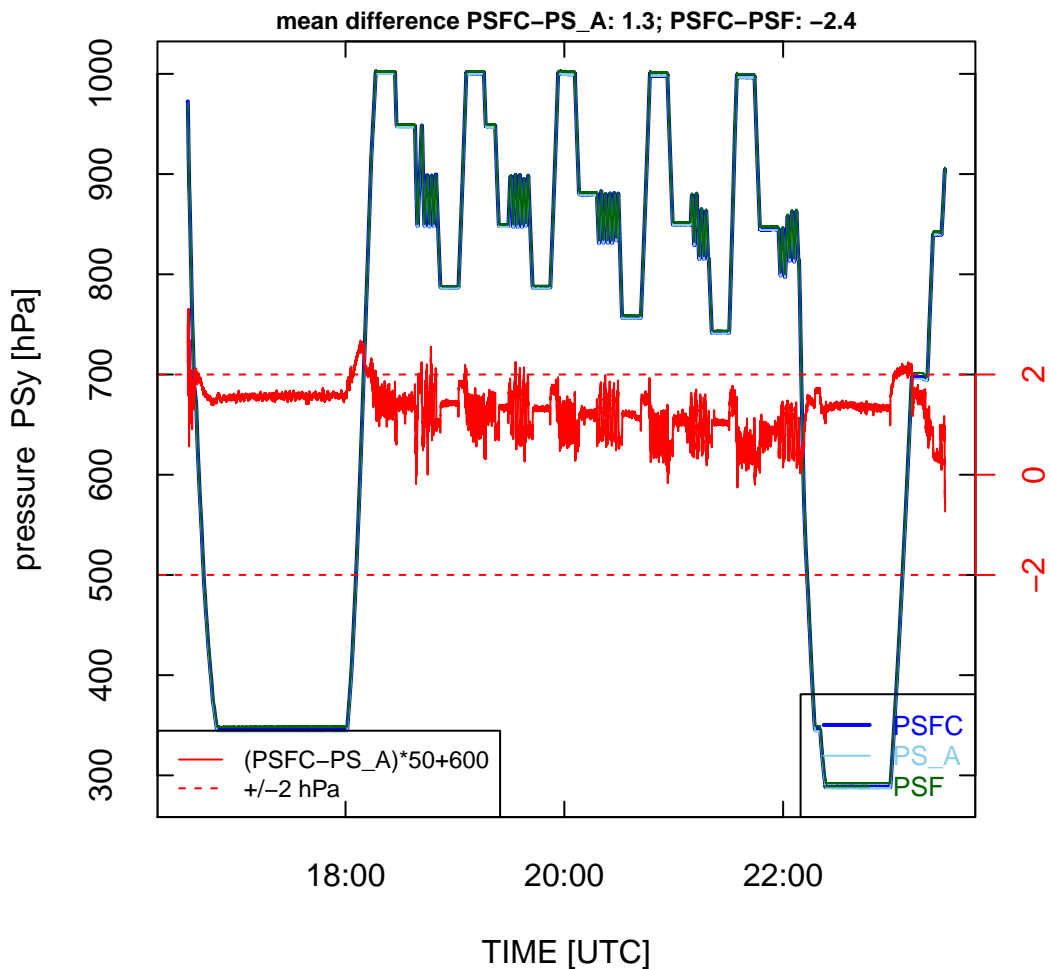
The differences between the mean values for the dew-point sensors (listed in the title of the plot) should usually be less than about 0.5°C.

The second plot (Fig. 6) compares the measurements to one selected as a reference, here DP_VXL. The overshoot problem appears in this plot in the extension to high dew point, above 25°C, values that appear unrealistic and are above anything measured by the UV hygrometer. The larger scatter of blue dots (DP_DPL) in this plot, in comparison to the red dots (DP_DPR), reflects the slower response of DP_DPL. This appears to be typical and acceptable behavior for the dew-point sensors on the GV. For dewpoint values below about -60°C, the dewpoint sensors are usually unable to respond, so for cases that include such values for DP_VXL it is common for the values of DP_DPL and DP_DPR to be too high.

Figure 7 shows the cavity pressures in the dew-point hygrometers. These are significantly below the ambient pressure, which is a result of their orientation on the aircraft. It would be preferable if that orientation provided a cavity pressure near or above ambient, because this reduction of pressure in the cavity reduces the range and response speed of the sensors. It is curious that the cavity pressure for DPR is much higher than that for DPL for ambient pressure near or above 800 hPa. However, the plot doesn't seem to indicate any problems with the measurements. The bottom panel of this plot shows the laser intensity for the VCSEL, which is expected to be between the two dashed red lines during normal operation.

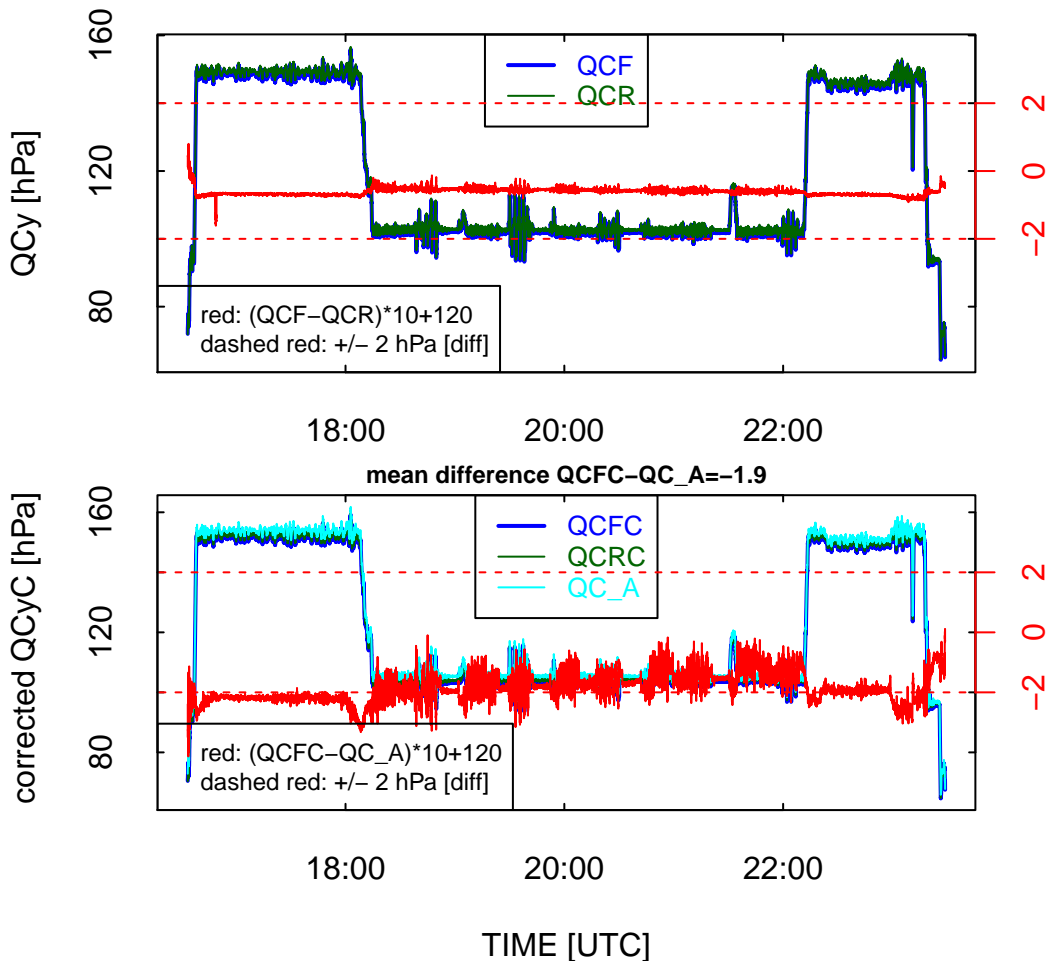
The final humidity plot, Fig. 8, shows the history of water vapor pressure, mixing ratio, and relative humidity from the various measurement systems. Excursions above relative humidity of 100% should be rare except in over-heating events like that near 18:15. The dashed cyan line in the top segment of this plot, labeled EW@ATX, shows the water vapor pressure that corresponds to equilibrium at the air temperature measured by ATX. In the top plot, the traces should almost overlap at the plot resolution for normal operation, except for very low water vapor pressures and overshooting regions (for the dew-point sensors). The mixing ratio plot and relative humidity plot show different perspectives on the humidity measurements.

Ambient or static pressure: Figure 9 compares the corrected measurement of static pressure, PSFC, to that provided by the avionic system (PS_A), and for reference also shows the uncorrected pressure measurement PSF. These plotted lines will usually almost completely overlap. The red line plots the difference, multiplied by 50 and offset by 600 hPa, as indicated by the red scale on the right axis. It is normal for PSFC to be higher than PS_A, but the measurements should not be offset more than about 1 hPa different in the range from FL290 – FL410 because this is the region covered by RVSM standards that PS_A must meet. This plot barely reaches that pressure range, but there the difference is outside expected limits. Corrections are being applied to PSFC based on the earlier LAMS calibrations, so it will be important to consider if something has changed those calibrations. (Measurements from the HCRTEST program in late 2014 showed a similar difference in comparison to LAMS results. It is also possible that the presence of the large pods has changed the required pressure corrections. For CSET, the best approach will be to check for consistency of this result from flight to flight and then depend on a new calibration, either from HCRTEST or ARISTO, to resolve the difference.



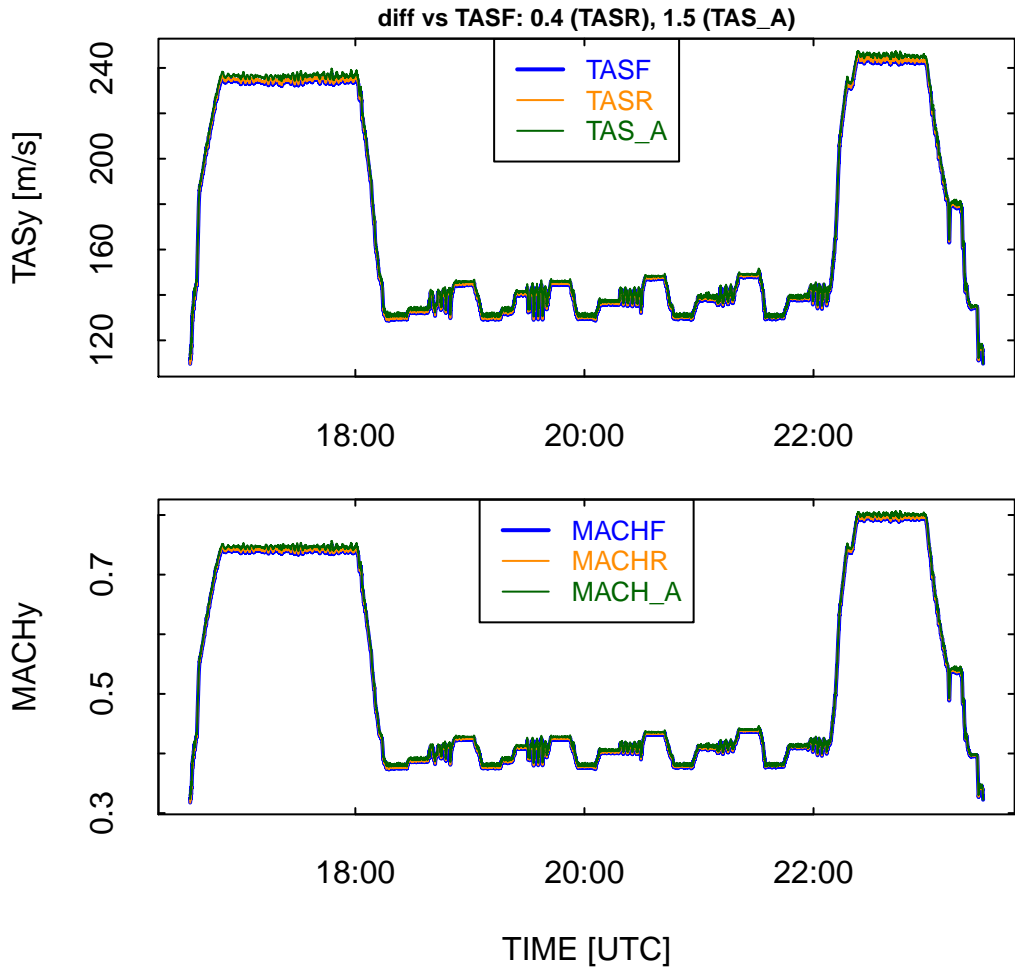
CSET RF03 2015-07-09 14:58:59-23:48:53 UTC, generated by RPlot6 2015-07-14 07:46:16 MD1

Figure 9: History of available pressure measurements, both uncorrected (PSF) and after application of the LAMS-derived pressure corrections (PSFC). The avionics-system pressure PS_A is also shown.



CSET RF03 2015-07-09 14:58:59–23:48:53 UTC, generated by RPlot7 2015-07-14 07:46:16 MD1

Figure 10: History of available measurements of dynamic pressure, both uncorrected (top) and after application of the LAMS-derived pressure corrections (bottom).



CSET RF03 2015-07-09 14:58:59–23:48:53 UTC, generated by RPlot7 2015-07-14 07:46:16 MD1

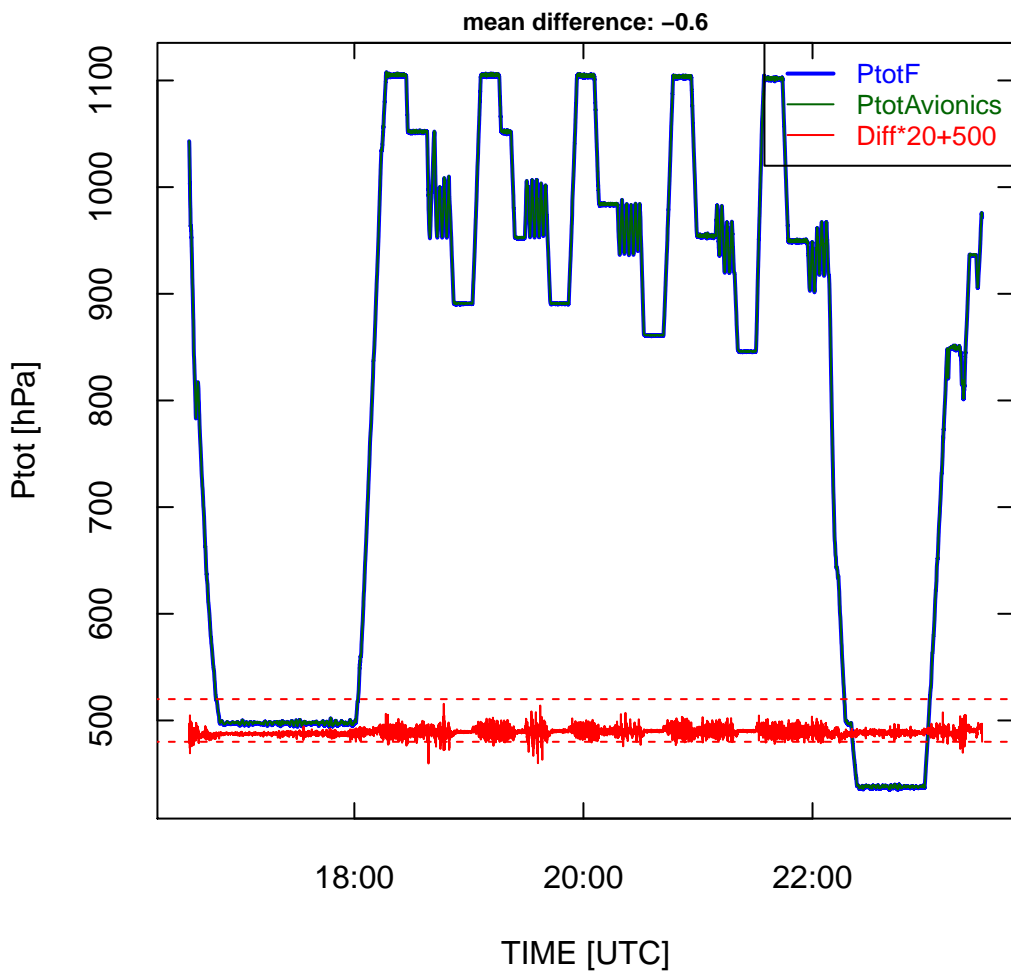
Figure 11: History of redundant measurements of true airspeed and Mach number.

Dynamic pressure: Measurements of dynamic pressure, similar to those from the ambient pressure, are shown in Fig. 10. The uncertainty in these measurements should be about 0.3 hPa, so the differences shown are large compared to expected differences and indicate a possible problem, in particular with QCFC. HCRTEST results from LAMS suggested that the airspeed measurement based on QCFC may be low by about 0.7–1.0 m/s (TASF). As for PSFC, it may be best to check for consistency with this pattern from flight to flight and then await a new calibration to resolve the apparent problem. and with QCFC. redundant sets QCFC and QCFRC (bottom panel) should agree within about this tolerance. As for PSFD and PSFRD, an offset is expected but that offset should remain consistent. Any significant change should be an indicator of a problem. An additional plot, Fig. 11, shows two measurements dependent on the dynamic-pressure measurements, TAS and MACH. TAS measurements normally should agree to within about 1 m/s, and the Mach lines normally overlap to about the resolution of the plot.

Total pressure: Adding the measurements of dynamic and ambient pressure gives the total pressure measured at the input of a pitot tube. The data-system value (P_{totF}) and the value from the avionics system are compared in Fig. 12. These usually should agree to within about 1 hPa, the limit shown by the red dashed lines. The mean difference shown here, -0.6 hPa, is larger than observed in past projects and another flag that the pressure measurements, while good, are not of the best quality possible and merit further attention.

Wind: The measurements of horizontal and vertical wind are shown in Fig. 13, and also in terms of easterly and southerly components in Fig. 14. Mean vertical wind averaged over the full flight should be close to zero, usually with absolute magnitude less than 0.3 m/s. The offset here is larger than normal and suggests a possible need for revision of the sensitivity coefficient for angle of attack. In CSET, the vertical-wind measurement has appeared to be somewhat inconsistent and will need further attention. The horizontal wind measurements can be used to check for reasonable continuity without excessive noise, although when the wind speed is weak there may be substantial noise in the WDC measurements. Wrap-around from 0 to 360 causes vertical lines in this plot that can be more frequent when the wind direction is near 0 or 360. For this reason, the second plot, showing easterly and southerly components, can be a better indicator of continuity. The faint green lines are measurements from the IRU alone and are expected to be of lesser quality than the wind measurements WSC and WDC, but large differences are not normal.

Ground-speed components (Schuler oscillation): The IRU measurements of ground speed will usually have some error that varies in a Schuler oscillation with a period of about 84 min. The magnitude of this oscillation is usually less than a few m/s, and in the wind calculations this oscillation is removed by adjustment to the GPS measurements, but excessive amplitude or unexpectedly noisy measurements can indicate a problem worth investigating. Figure 15 shows the difference between ground-speed measurements from the IRU and the GPS. The magnitude of the oscillation here is larger than typical; that from CSET flight 2 was much smaller in amplitude. This probably reflects a larger-than-normal error in initial alignment. These errors do not have much effect on the



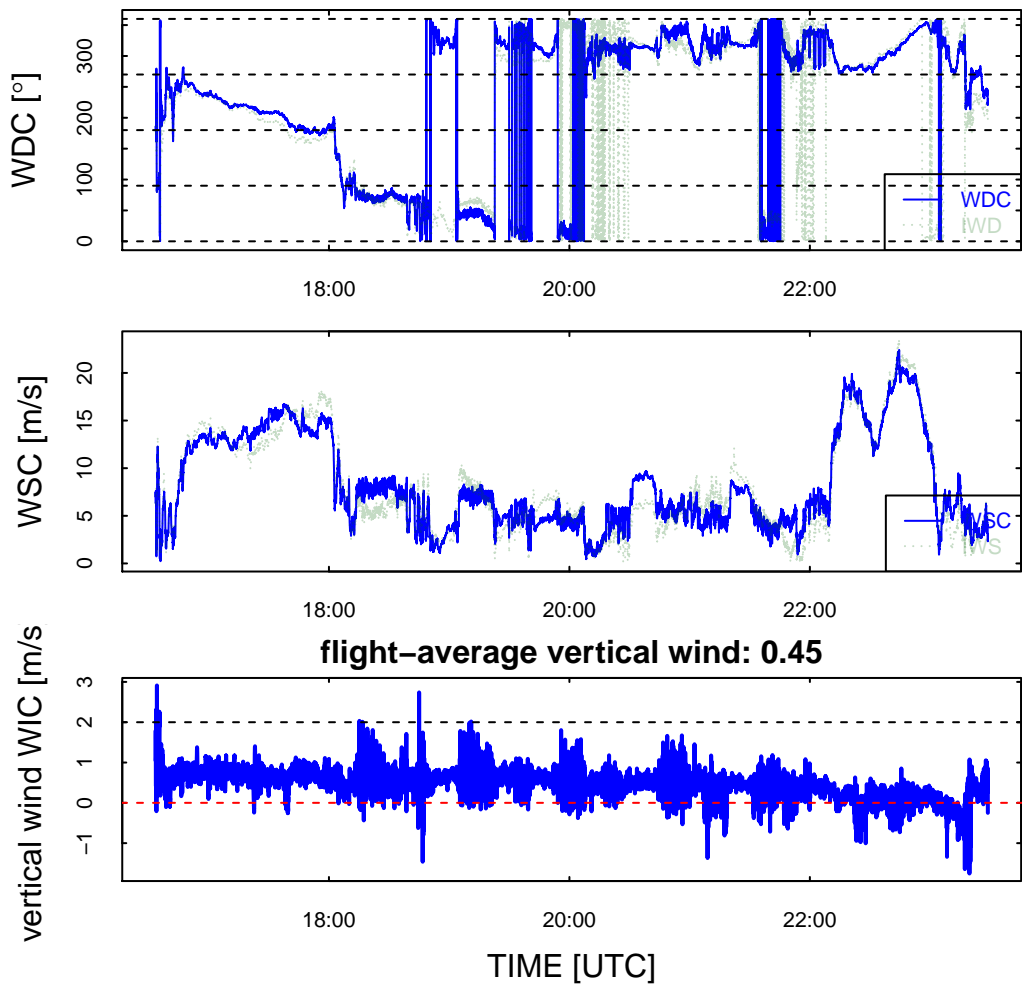
CSET RF03 2015-07-09 14:58:59–23:48:53 UTC, generated by RPlot8 2015-07-14 07:46:16 MD1

Figure 12: Total pressure measurements obtained by adding the independent pairs of measurements PSFD+QCF and PSFRD+QCFCR (i.e., the uncorrected measurements). Exactly the same plot is obtained for the corrected measurements because the pressure-correction function is applied to pairs of PS and QC measurements with opposite sign, positive for PS and negative for QC.

Memo to: CSET data-processing file

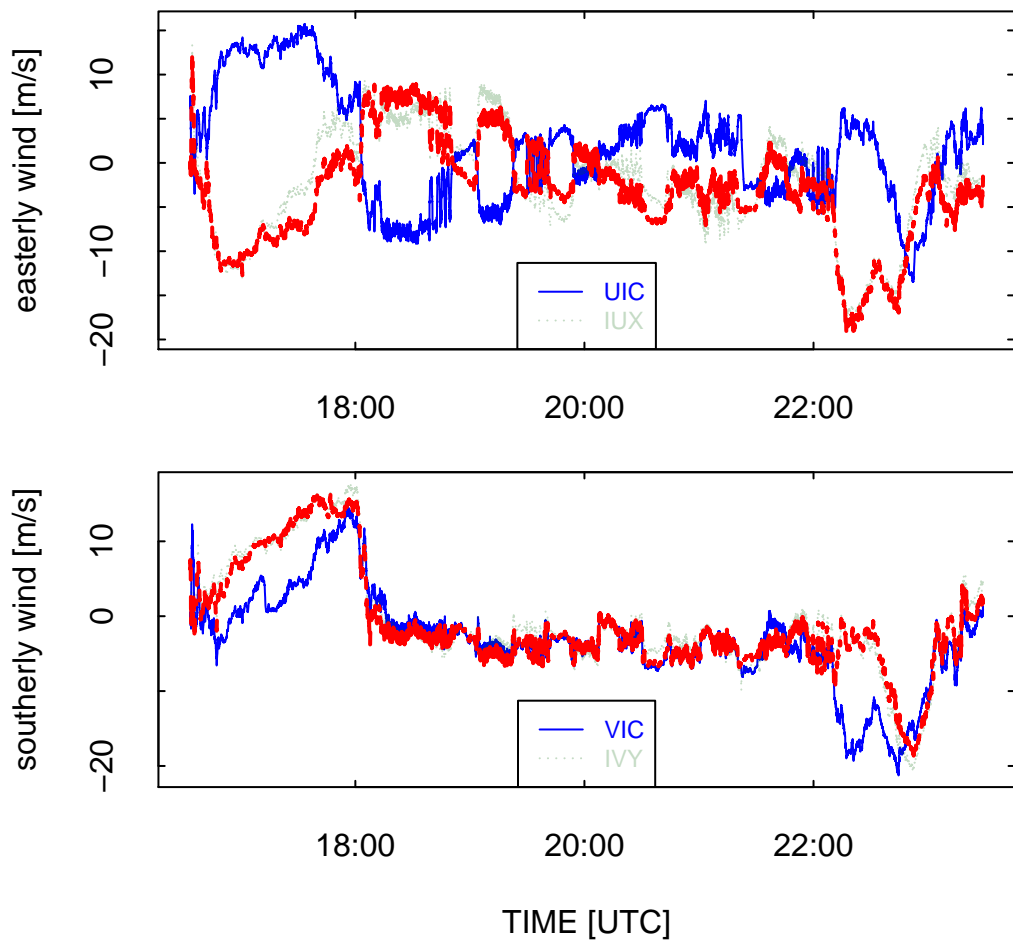
14 July 2015

Page 18



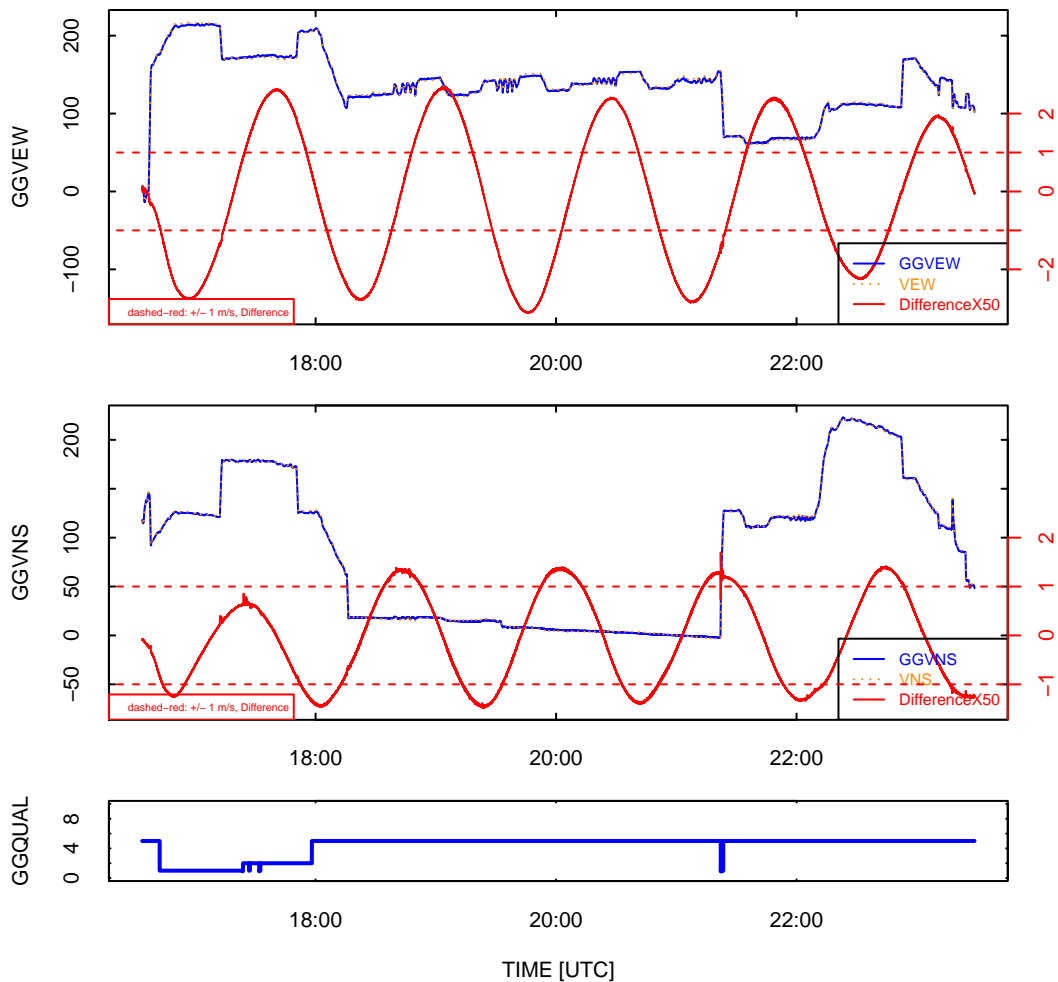
CSET RF03 2015-07-09 14:58:59–23:48:53 UTC, generated by RPlot9 2015-07-14 07:46:16 MD1

Figure 13: History of wind measurements, horizontal (WDC/WSC) and vertical (WIC). See the next plot for the horizontal wind plotted in terms of easterly and northerly components.



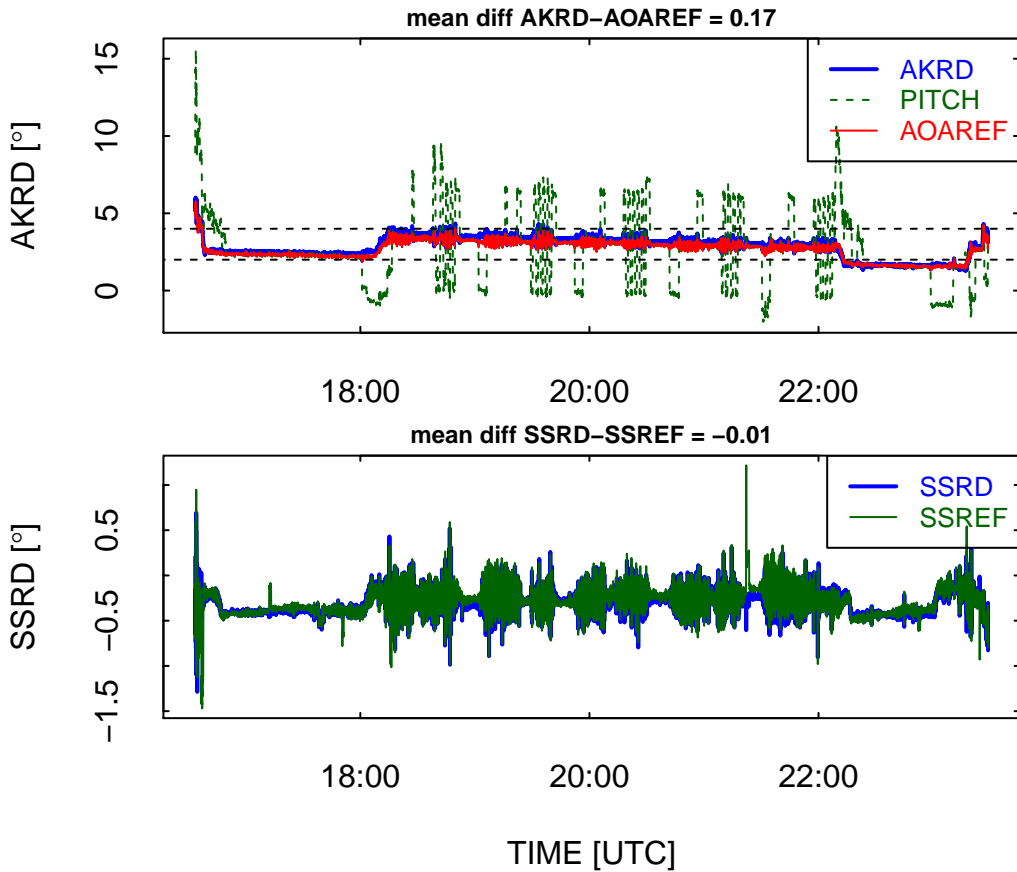
CSET RF03 2015-07-09 14:58:59–23:48:53 UTC, generated by RPlot9 2015-07-14 07:46:16 MD1

Figure 14: Westerly and northerly components of the horizontal wind, as shown in the previous plot in terms of direction and speed.



:SET RF03 2015-07-09 14:58:59–23:48:53 UTC, generated by RPlot10 2015-07-14 07:46:16 MD

Figure 15: Comparison of ground-speed components measured by the GPS and IRU units (blue and dashed orange lines), along with the difference (red line). Dashed red lines show ± 1 m/s limits.



:SET RF03 2015-07-09 14:58:59-23:48:53 UTC, generated by RPlot11 2015-07-14 07:46:16 MD

Figure 16: Measurements of the angles of attack and sideslip (blue traces, [deg.]), plotted with the reference values used for calibration that depend on the assumption of zero vertical wind or zero real sideslip not caused by wind gusts.

final horizontal-wind measurements, but they are associated with errors in pitch and roll that can affect the vertical wind. The lowest panel in this plot shows the value of GGQUAL, which will be 5 for OmniStar reception from the Novatel GPS receiver, indicating highest-quality measurements.

Angles of attack and sideslip: The sensitivity coefficients for angle of attack and sideslip are determined using reference values of attack and sideslip (here plotted as AOAREF and SSREF) that would be valid measures of the angles of attack and sideslip if there were respectively zero vertical wind and zero sideways wind gust.

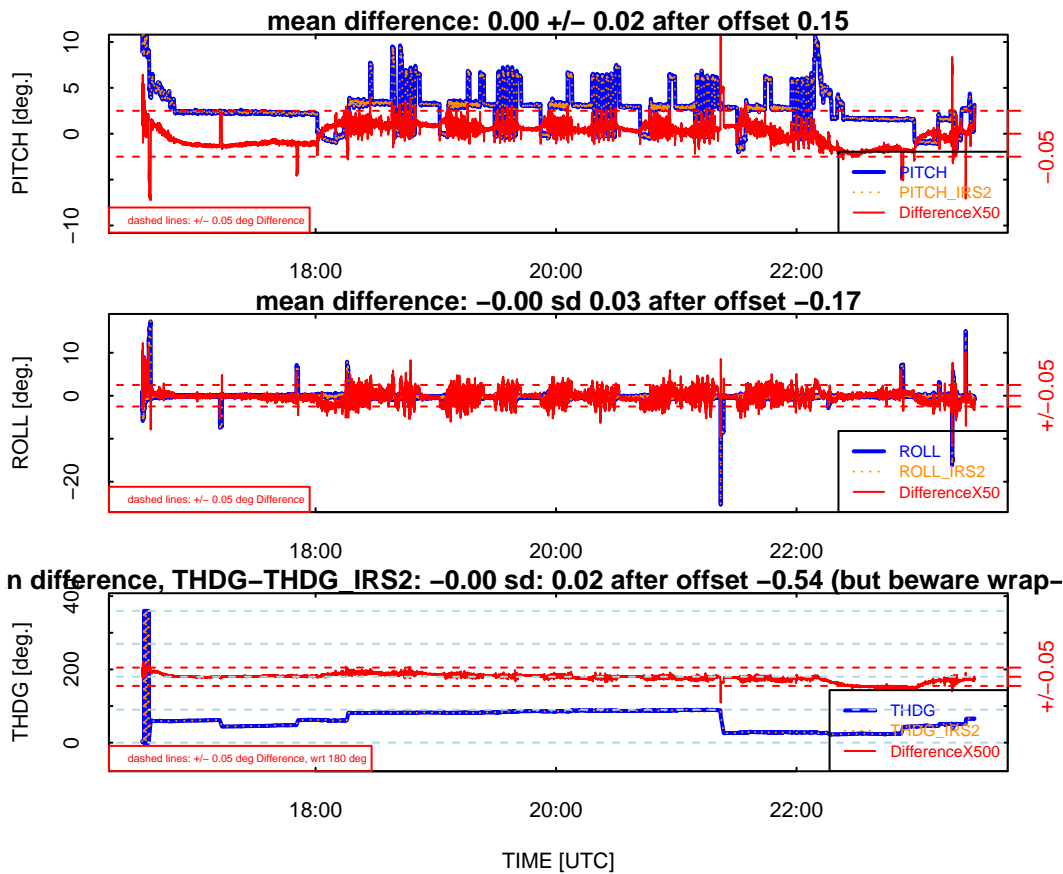
Figure 16 shows a comparison of the measurements to the reference values. If the calibration is valid, the blue and red traces in the top plot and the blue and green traces in the bottom plot should match in the mean, with occasional fluctuations caused by real wind gusts. PITCH is also shown in the top plot because, in the absence of both vertical wind and aircraft climb or descent, the pitch

would match the angle of attack. For the GV, the usual angle of attack is about $3 \pm 1^\circ$, so these limits are denoted on the top panel. Notice the gradual decrease in angle of attack during the course of the flight; this is normal behavior as the weight of the aircraft decreases. Agreement in the mean between AKRD and AOAREF is a good indication that the radome calibration is valid. This is useful to monitor because there have been some unexplained changes in radome behavior, perhaps from changes in mounting alignment or from flow interference from small accretions of dirt near the radome ports. The example plot shown for research flight 3 shows disagreement between AKRD and AOAREF at about the limit that should be acceptable, because an angle-of-attack error of 0.17° would result in a vertical-wind error (at TAS=140 m/s) of about 0.4 m/s, similar to the mean offset measured in the vertical wind for this flight. In this case, the sideslip matches the reference values very well.

Aircraft attitude angles: pitch, roll, heading The research IRUs provide redundant measurements of the attitude angles, so comparing them tests if they remain consistent. They should agree to within about 0.05° except for possible errors in alignment when the units are installed in the aircraft.

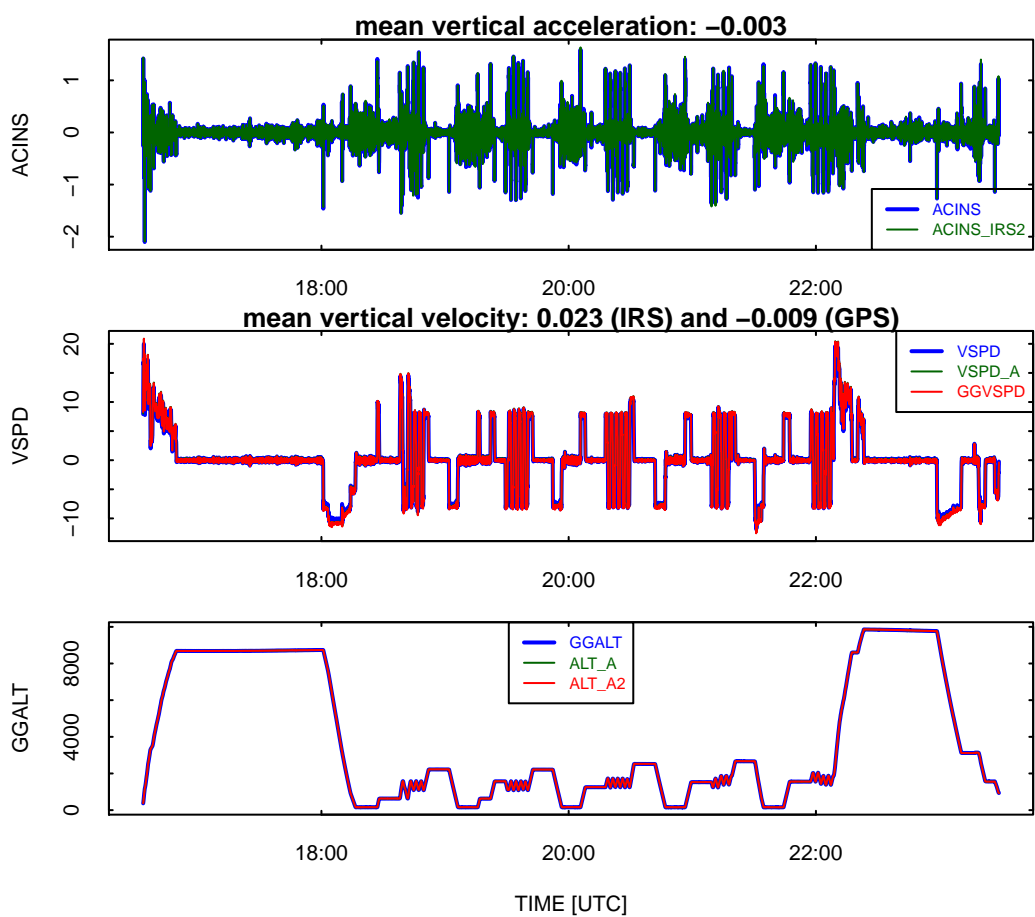
Figure 17 shows the measurements from the two inertial systems and also a magnified (red) plot of the differences between the two units (IRS1 value minus IRS2 value). Dashed red lines show the expected tolerances for these magnified differences. The dashed red lines provide guidance; normal operation should produce red lines than lie within the dashed red lines in each plot. For pitch, typical values are about 3° as expected but the difference between the two units is 0.15° , much larger than expected. The offset for research flight 2 was similar. This appears to be a difference between how the two units are installed, because the standard deviation of that difference is quite small, about 0.02° . Because this is so steady for this flight, it is probably an indication of a real difference in alignment, which should be considered if the primary unit used for wind calculations is changed. For CSET the mean differences in all angles (IRU1-IRU2) are about -0.15° , $+0.17^\circ$, and $+0.54^\circ$ for, respectively, pitch, roll, and heading, so these values have been subtracted from the difference plots. The corresponding values for DEEPWAVE were -0.20° , $+0.19^\circ$, and $+0.49^\circ$. These are reasonably consistent but suggest small changes in the relative orientation of the two IRUs between these two projects..

Vertical acceleration, vertical velocity of the aircraft, and aircraft altitude Figure 18 provides additional information on the performance of the INS and GPS systems. The top panel shows a comparison of the measurements of vertical acceleration; these should match to strict tolerance because the acceleration is integrated twice to get the altitude. The difference, shown here as -0.003 , should be less than about 0.01 in magnitude for normal good operation of the inertial units. This does not have to be exactly zero because the data used are qualified to have TASX > 110, so some brief periods near the start and end of flights can be omitted. The middle panel shows the vertical speed of the aircraft as measured by three independent systems. All are in good agreement, and the flight-mean values are 0.023 and -0.009 m/s respectively for the inertial and GPS-Novatel units. The mean velocity should be very close to zero for a flight that takes off



:SET RF03 2015-07-09 14:58:59-23:48:53 UTC, generated by RPlot12 2015-07-14 07:46:16 MD'

Figure 17: Comparison of attitude angles measured by the two duplicate research inertial systems on the C-130, with dashed reference lines indicating the uncertainty limits quoted by the manufacturer for the angle measurements. The red lines show the differences multiplied by 50 for pitch and roll and by 500 for heading, with a further offset of 180° for heading to center the difference plot.



CSET RF03 2015-07-09 14:58:59-23:48:53 UTC, generated by RPlot13 2015-07-14 07:46:16 MD

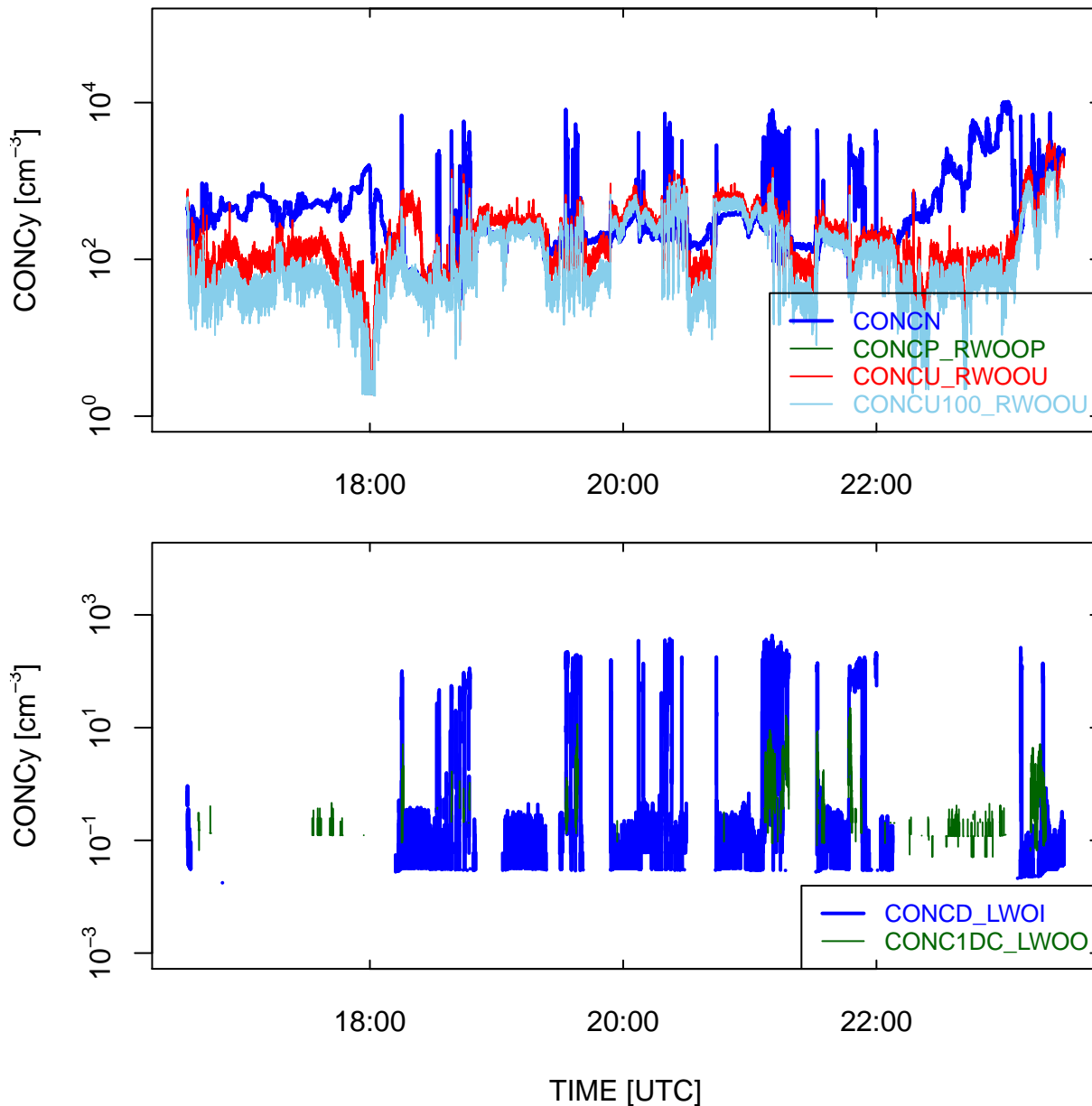
Figure 18: Vertical acceleration (top), vertical aircraft velocity (middle), and aircraft altitude (bottom) for the available redundant measurements.

and lands at the same airport or at the same geometric altitude. These values, esp. that for the IRS, are larger than normal: The uncertainty associated with GGVSPD is about 0.03 m/s, which for a flight of about 7 h would integrate (if always of the same sign) to an error in altitude of about 750 m, so this is an extreme value larger than expected. The observed means for VSPD and GGVSPD seem reasonable in comparison to other flights. The bottom panel will normally show the three measurements of altitude from independent systems overlapping so much as to be indistinguishable. In this case, if there are occasional spikes in the altitude from the Novatel GPS, as observed in some previous projects, that will indicate a problem needing investigation. Here there is no indication of a problem.

CN, UHSAS, CDP, and 2DC concentrations The plots in this section show measurements from particle and hydrometeor distrometers on the GV. The top panel of the first figure, Fig. 19, shows the CN concentration along with two concentrations from the UHSAS, the red trace representing the total concentration and the sky-blue trace denoted the concentration of particles larger than $100 \mu\text{m}$ in diameter. (PCASP, listed in the legend as CONCP, is a remnant from the test flights and is not present for this flight. The bottom panel shows concentrations from the CDP and the 2DC. The apparent floor on the plot of CDP concentration arises because that is the threshold for a single droplet counted in the 1-s interval used for these measurements. Zero values are reset to missing for these log plots. CDP concentrations of order $100/\text{cm}^{-3}$ are expected in water cloud; and should correlate with measured liquid water content from the King probe (shown below). CDP concentrations of a few tenths/ cm^{-3} result mostly from detection of aerosols. The 2DC concentration should remain zero in cases of flight outside cloud, as it does except for a few brief bursts (green lines). A steady 2DC concentration above zero in clear air may indicate a problem with the uniform illumination of diodes or a bad diode in the instrument.

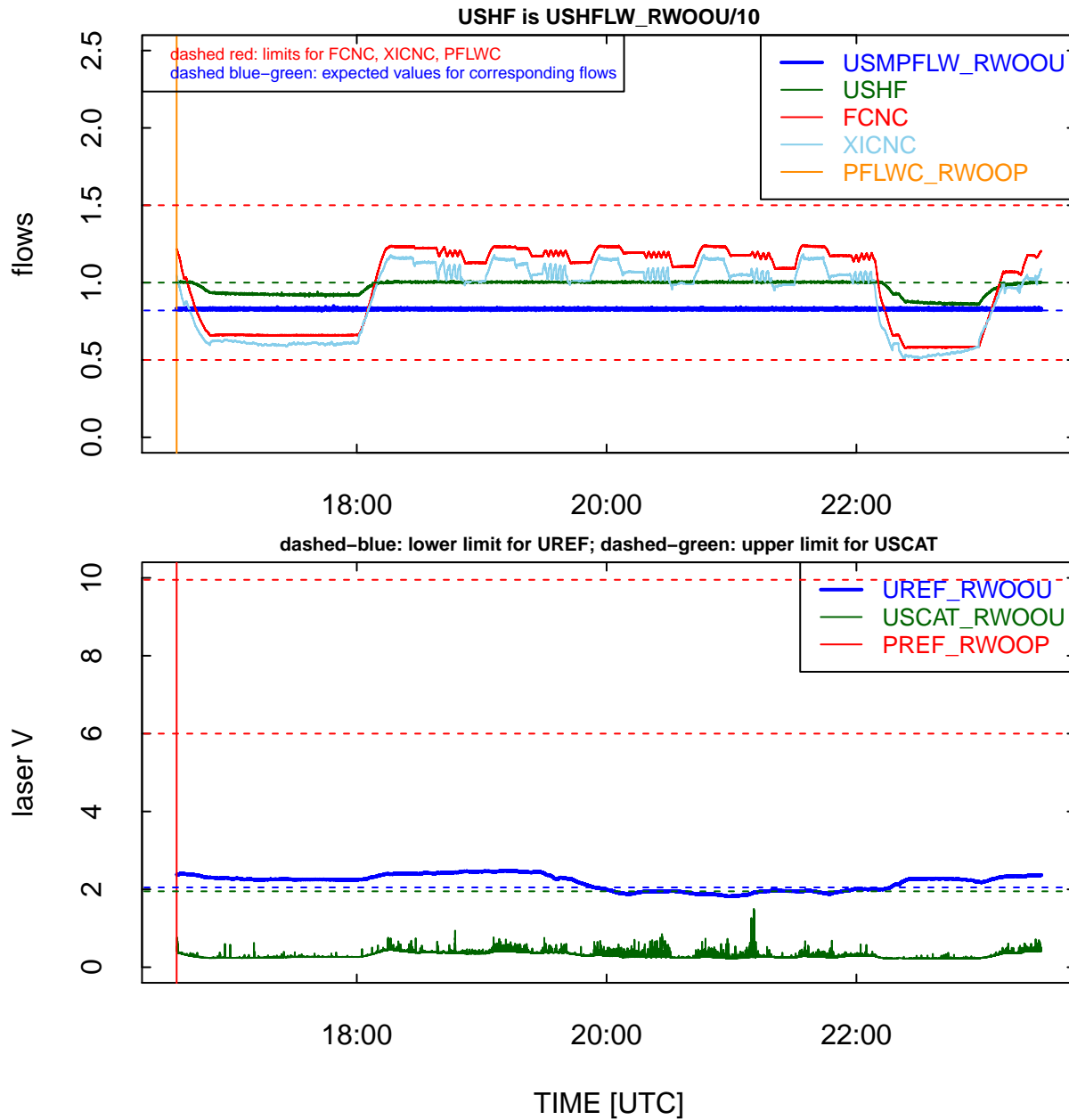
The next plot, Fig. 20, shows some housekeeping measurements useful for monitoring the status of the particle-measuring instruments. In the top panel, the blue trace (USMPFLW) and the green trace (USHF) are respectively the flow and sheath flow in the UHSAS, both expected to be in the range 0.8–1.0 as indicated by the blue-green dashed lines. FCNC and XICNC are respectively the sample flow and isokinetic side-flow in the CN counter, expected to be in the range indicated by the dashed red lines. The orange line represents the PCASP flow and will not be present while, as for this flight, the PCASP is not installed on the aircraft. The bottom panel shows some laser monitoring variables, UREF that for the UHSAS (expected to be above the dashed blue line), USCAT for the UHSAS background scatter (expected to be below the dashed green line), and PREF for the PCASP (here not present but expected to be between the dashed red lines if present).

Mean diameters and liquid water content of hydrometeors Figure 21 shows measurements of the mean diameters measured by the CDP, UHSAS, and 2DC. These measurements and those of liquid water content can be quite noisy and therefore hard to interpret, so this plot and the next one have been smoothed over running periods of 61 s using cubic Savitzky-Golay polynomials. That led to much smoother plots that are easier to interpret, but at the expense of losing fine resolution in cases of short passage through clouds. For that reason, this plot and the others in this section are



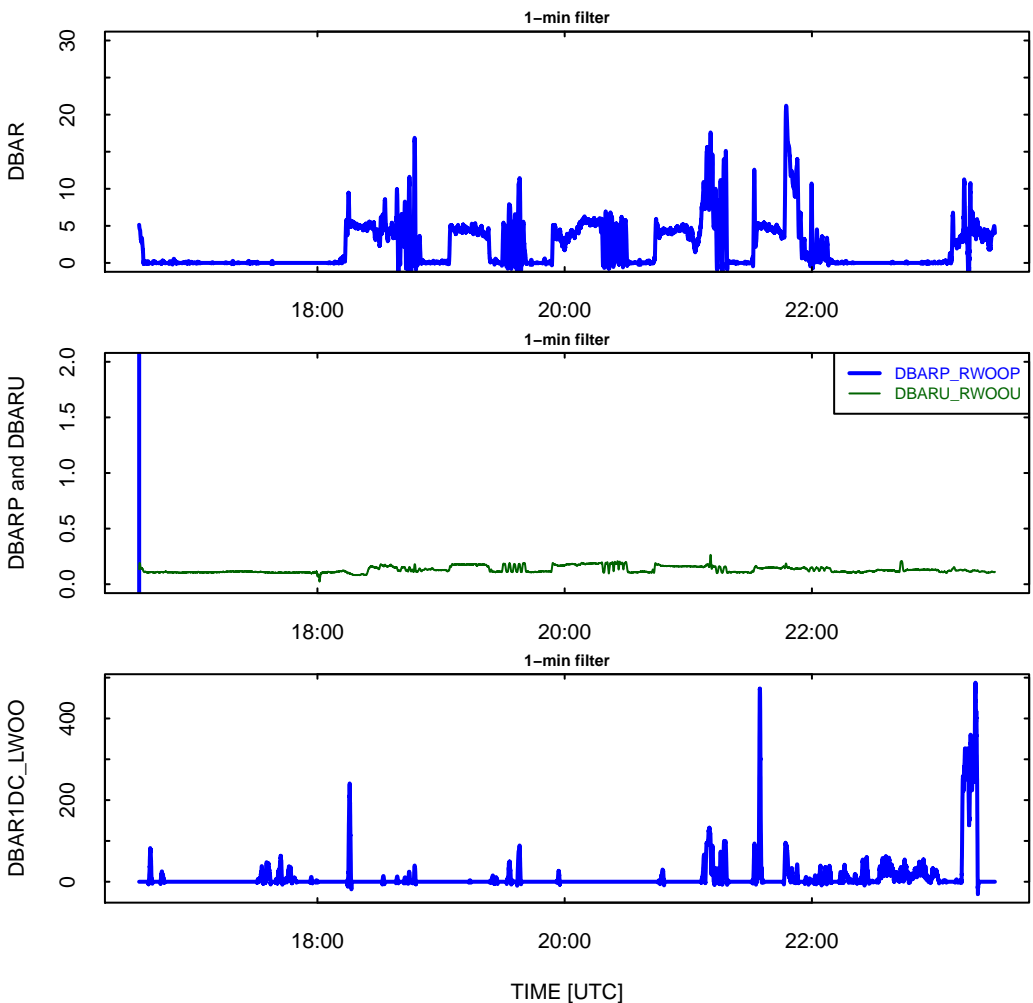
CSET RF03 2015–07–09 14:58:59–23:48:53 UTC, generated by RPlot15 2015–07–14 07:46:16 MDT

Figure 19: (top) Particle concentrations from the CN counter, UHSAS (all and larger than 100 nm) and PCASP aerosol distrometer if available, and (bottom) hydrometeor concentrations from the CDP and 2DC with 2DC shown in units of liter^{-1} .



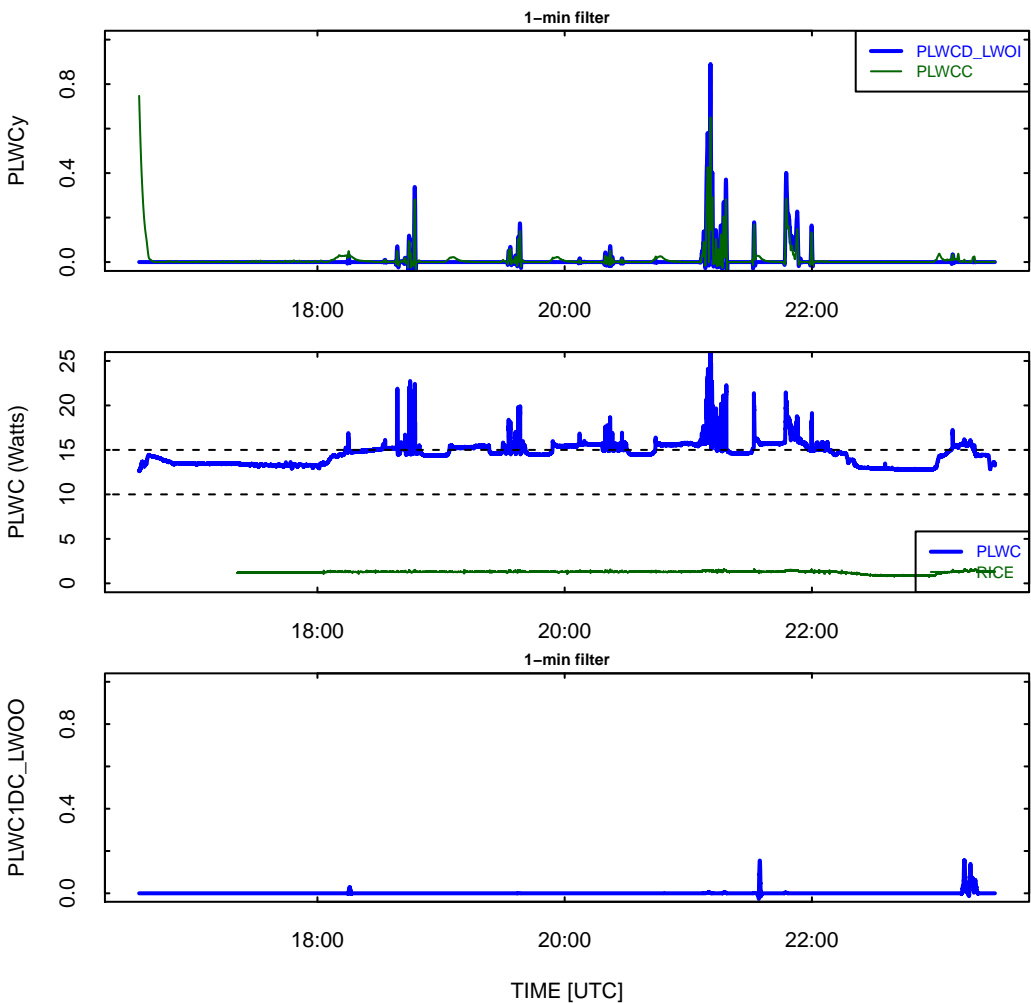
CSET RF03 2015–07–09 14:58:59–23:48:53 UTC, generated by RPlot15 2015–07–14 07:46:16 MDT

Figure 20: Housekeeping measurements useful for monitoring the status of the particle-measuring instruments. (top) USMPFLW and USHF, respectively the flow and sheath flow in the UHSAS; FCNC and XICNC, respectively the sample flow and isokinetic side-flow in the CN counter, and (if present) PFLWC, the flow in the PCASP. (bottom) UREF, monitoring the laser voltage in the UHSAS, and USCAT, measuring the background scatter in the UHSAS. If the PCASP is present, PREF monitors its voltage.



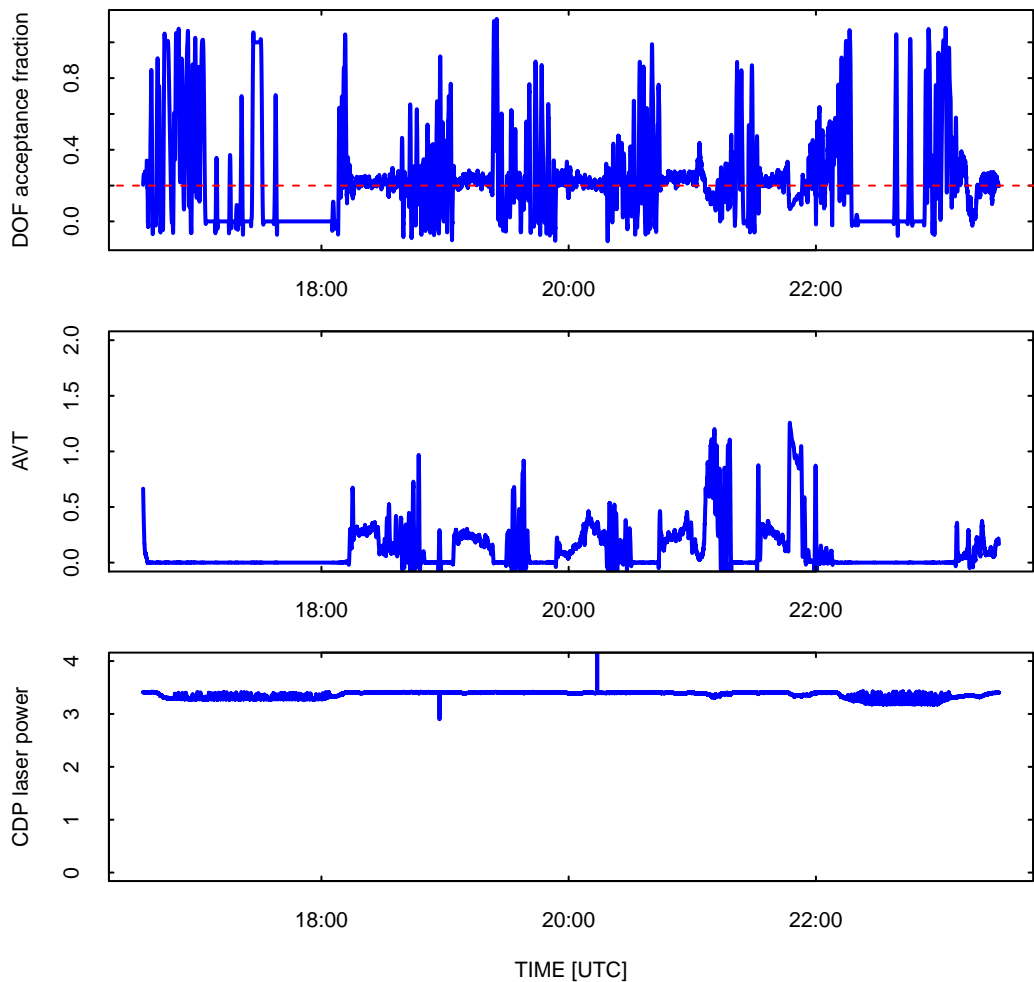
:SET RF03 2015-07-09 14:58:59–23:48:53 UTC, generated by RPlot16 2015-07-14 07:46:16 MD

Figure 21: Mean diameters [μm] measured by the CDP (top), the UHSAS (and PCASP if available) (middle), and 2DC [bottom].



:SET RF03 2015-07-09 14:58:59-23:48:53 UTC, generated by RPlot16 2015-07-14 07:46:16 MD

Figure 22: Measurements of liquid water content from the CDP and King probe (top); the power required to maintain King-probe temperature (middle), and the estimated liquid water content from the 2DC probe with the assumption that all particles are liquid.



:SET RF03 2015-07-09 14:58:59–23:48:53 UTC, generated by RPlot16 2015-07-14 07:46:16 MD

Figure 23: Additional characteristics of the CDP: percentage of DOF-accepted particles (top), average transit time (middle), and the laser power (bottom).

likely only useful for data-quality review, not for analysis conclusions.

The mean diameter shown in the top panel of Fig. 21 shows reasonable behavior for the CDP for low-level clouds where droplet sizes are expected to be small. For the UHSAS, the measurements are dominated by particles in the smallest-size channels; this appears suspicious to me, and it is more common to see more variation than this in the UHSAS mean diameter, but the size distributions (shown below) seem reasonable so I'm not sure there is a problem. The mean diameters measured by the 2D seem reasonable and show a brief period of larger-droplet measurements near the end of the flight.

The same smoothing is applied to the liquid water content measurements shown in the top panel of Fig. 22. The regions with liquid water content from the CDP (PLWCD) are reasonably consistent in location and magnitude with the liquid water content from the King probe (PLWCC), except in some cases where altitude changes caused excursions on PLWCC not present in PLWCD. The power from the King probe is shown in the middle panel, as PLWC; this is normally in the range from 10–15 watts except when encounters with liquid water require more power to maintain the constant temperature of the sensing wire. The bottom panel shows the liquid water content from the 2DC probe, which measured only very small amounts on this flight but may be higher in cases with well-developed warm rain.

In addition, some housekeeping information is shown in Fig. 23, including the DOF acceptance ratio (typically about 0.2), the average transit time AVT and the CDP laser power, typically above 3.

Plots on a thermodynamic (skew-T) diagram Skew-T diagrams can indicate problems if they show regions where the temperature decreases with altitude faster than expected for parcel ascent, and they can also indicate layers of strong stability where boundary-layer pollution may be trapped. They can also indicate the potential for the development of clouds and the potential for severe weather. A skew-T plot is included here (Fig. 24 for information and context, but as long as the appearance resembles this plot it will probably not add to the quality-control information. There is also a section of this program, suppressed in the project configuration, that searches for climbs and descents and constructs separate plots for them. Include 18 in the sequence named 'nplots' to see these individual plots. They are suppressed in this memo and the standard plots for CSET. There is a separate document that describes this skew-T diagram, which is based on the Davies-Jones values for pseudo-adiabatic equivalent potential temperature and on the Murphy-Koop formula for water vapor pressure.

Potential temperature histories and profiles Figure 25 shows the history of measurements of various potential temperatures during the flight, and Fig. 26 shows the same measurements in vertical profile. The latter can be useful because it is expected that potential temperature (THETA or THETAV) will normally decrease or remain steady as the altitude increases, and uniform regions indicate possible well-mixed regions such as in the Earth's boundary layer, often capped by modest stability reflected in increasing THETA. Virtual potential temperature (THETAV) exceeds

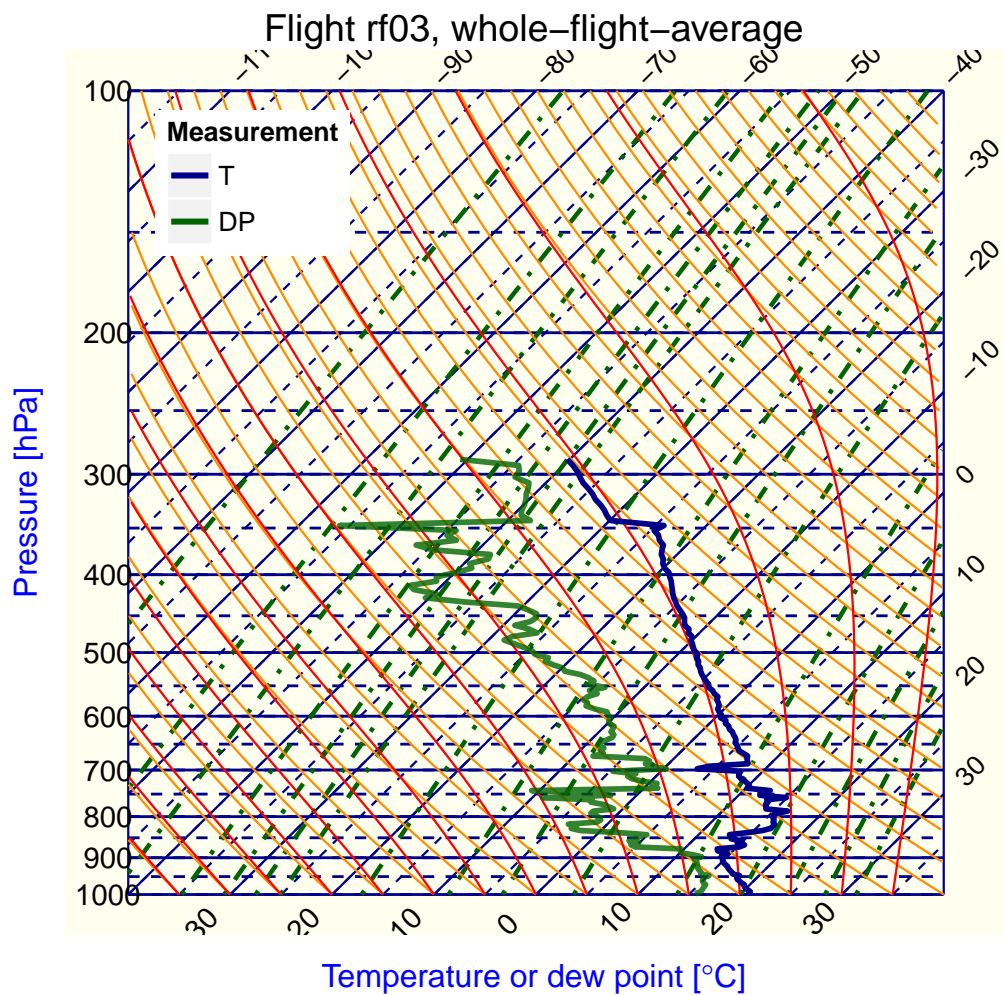
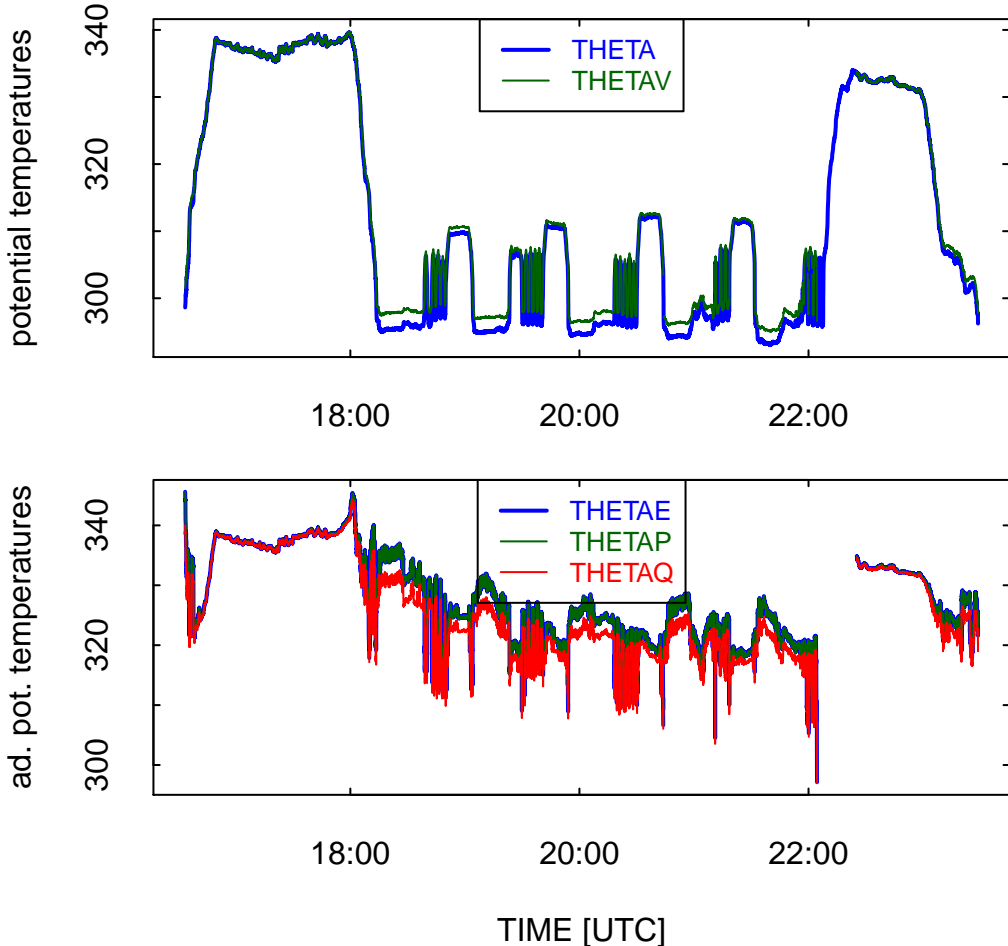
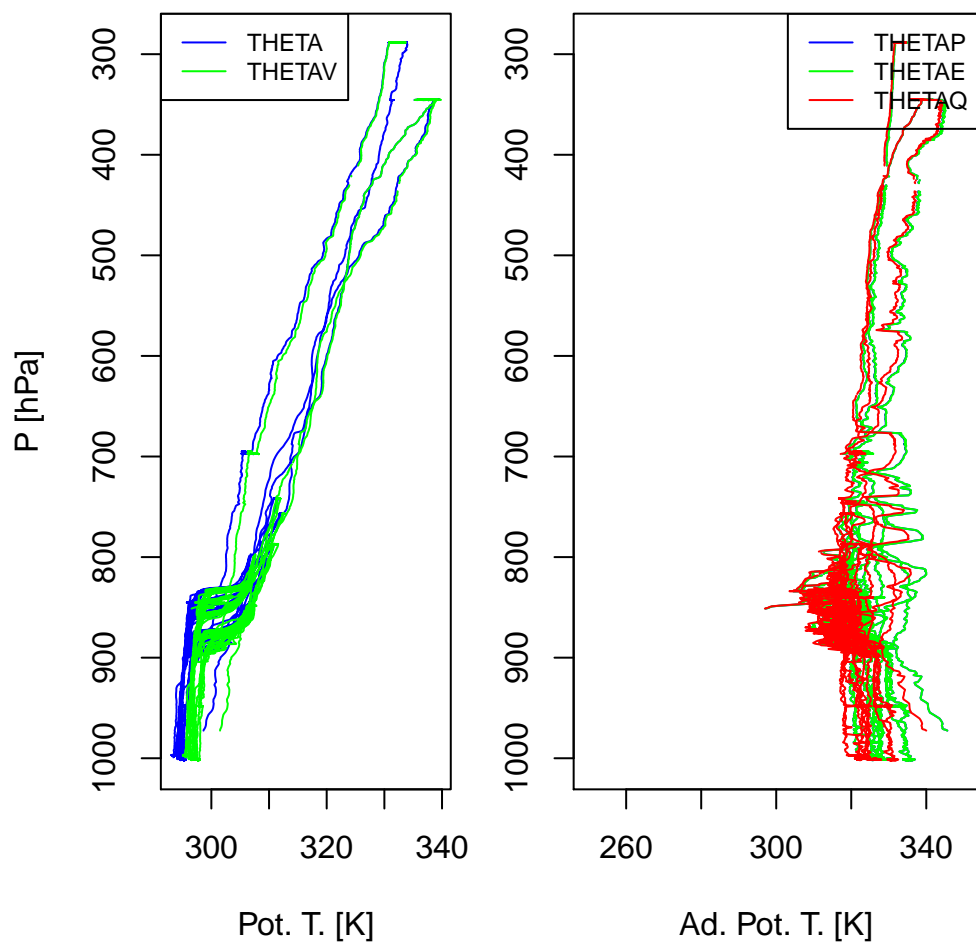


Figure 24: Plot of all temperature and pressure measurements, averaged in 5 hPa intervals, for the flight. The only restriction on data is that only measurements where TASX exceeded 110 m/s were used.



:SET RF03 2015-07-09 14:58:59-23:48:53 UTC, generated by RPlot19 2015-07-14 07:46:16 MD

Figure 25: Measurements of potential and virtual potential temperature (top panel) and of Bolton-formula equivalent potential temperature (THETAE), Davies-Jones pseudoadiabatic potential temperature (THETAP), and wet-equivalent potential temperature (THETAQ). All units are kelvin.



CSET RF03 2015-07-09 14:58:59–23:48:53 UTC, generated by RPlot19 2015-07-14 07:46:16 MD

Figure 26: Vertical profiles of the same measurements shown in the preceding figure.

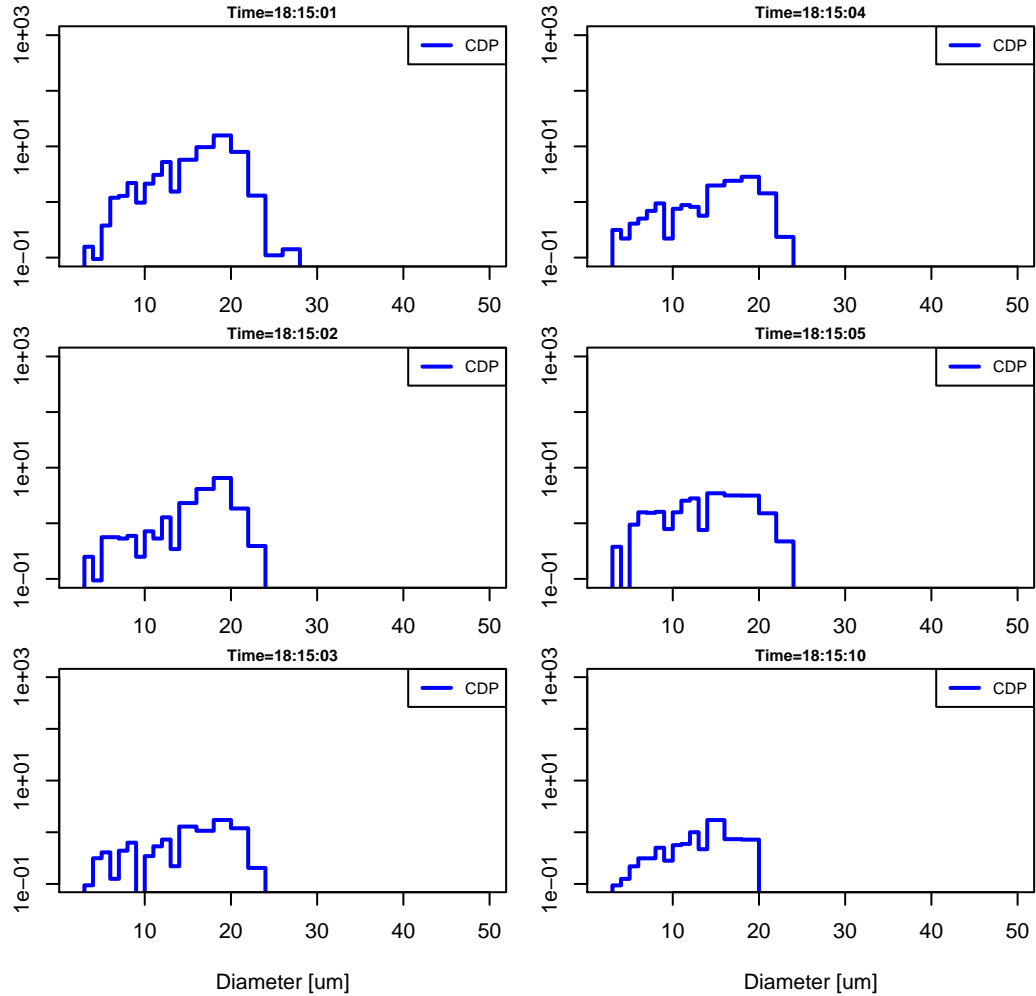
potential temperature (THETA) by an amount that increases with the water vapor mixing ratio, so plots normally look like Fig. 25 with large differences at low level but small differences at upper levels. The values THETA_E and THETA_P are different values of the pseudo-adiabatic equivalent potential temperature, based respectively on the Bolton and Davies-Jones equations, and THETA_Q represents the wet-equivalent potential temperature that would characterize true reversible ascent or descent. Where measurements of humidity are invalid or set missing, there will be gaps such as that appearing after 22:00 in this plot. The profiles often will show multiple lines because all individual measurements are plotted in connected lines, so for example there may be one plot for ascent and one for descent. Much more can be deduced by using profiles like these, but for the purposes of data review the best test is to expect plots resembling these and investigate departures. In Fig. 26, right side, the fluctuations in THETA_P or THETA_E with height in the range from about 800–700 hPa reflect fluctuations from passage into and back out of clouds during descents through these regions. Features like these should be investigated if they haven't been understood from the preceding plots.

Hydrometeor size distributions Size distributions measured by the CDP are shown in the next set of plots beginning with Fig. 27. Individual plots show measurements made over 1-s, as labeled at the top of the plots, and plots are only generated when at least one channel in the CDP measures a concentration of more than 1 cm^{-3} . Once three pages of plots are generated, the plotting is suppressed, so this only provides an initial limited sample, but it can be a useful indicator of acceptable CDP performance if the size distributions resemble those shown in this example.

Radiometric measurements The next plot, Fig. 31, shows the measured Earth-surface temperature (RSTB) and the infrared irradiances for down-welling (IRTC) and up-welling (IRBC) radiation. There will usually be reasonable correlation between RSTB and IRBC, and IRTC will usually drop to low values (<100) for flight at altitudes above FL300 unless there are thick Cirrus clouds above that altitude.

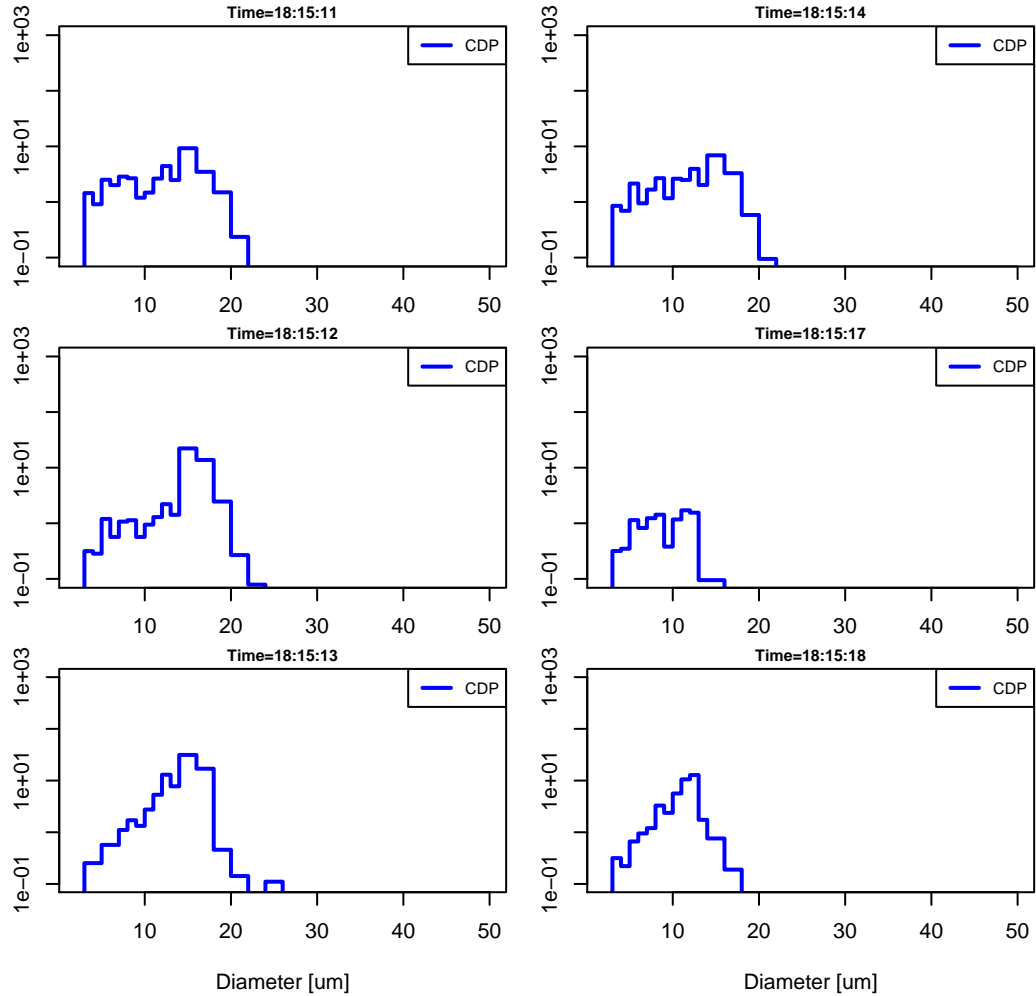
Aerosol size distributions Size distributions measured by the UHSAS are shown in a set of figures beginning with Fig. 32. These plots are only generated when some channel in the UHSAS has a concentration exceeding 50 cm^{-3} , and once 24 size distributions are plotted further plots are suppressed so these plots only show a snapshot of UHSAS performance. Review.R can be run with a specified time range to see other portions of the flight for these and other plots.

Air-chemistry measurements Figure 36 shows the history of measurements of CO and O₃ [ppbv], and Fig. 37 displays the inlet pressure of the Aerolaser CO instrument [units are torr, equal to about 1.333 hPa]. The last plot should also show the flow in the Aerolaser CO instrument, but for this flight and many of those preceding it all those values have been missing or not showing reasonable values, so this is left in the routine in case that problem is fixed in later flights.



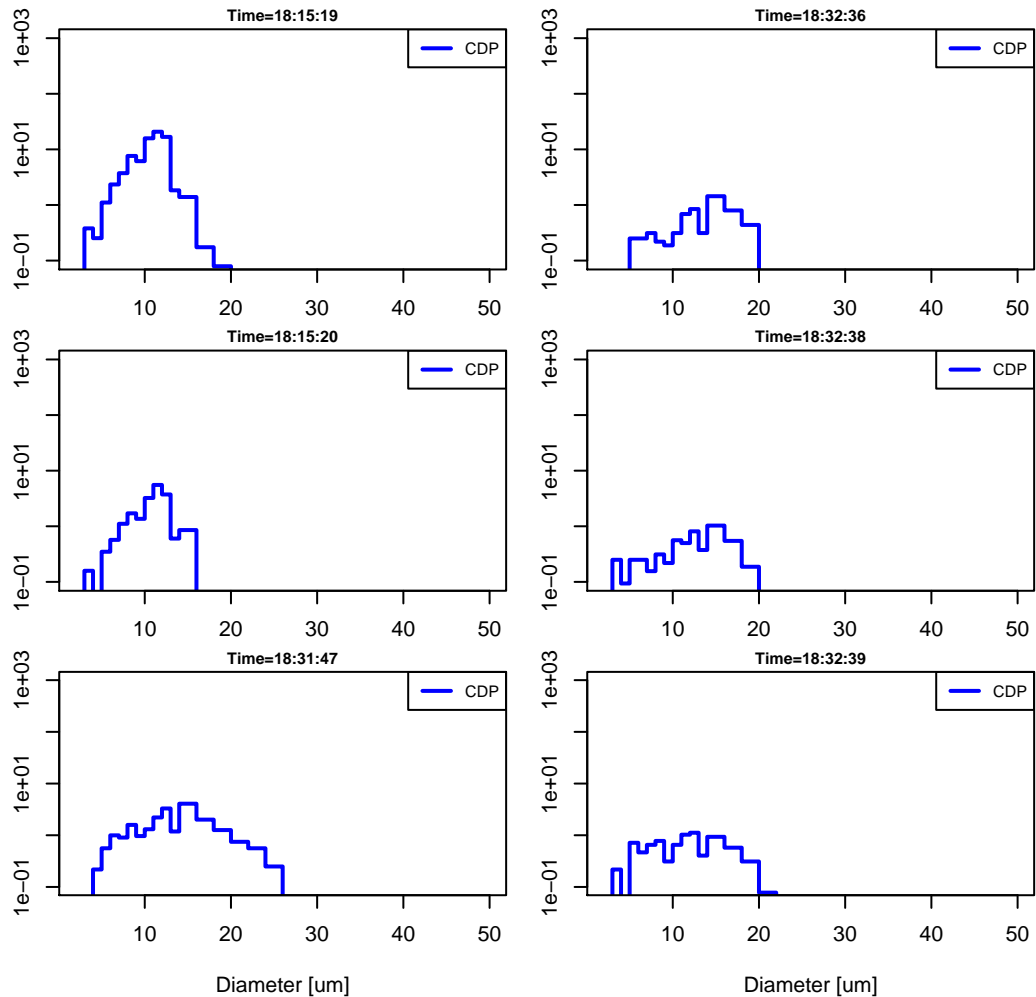
CSET RF03 2015-07-09 14:58:59–23:48:53 UTC, generated by RPlot20 2015-07-14 07:46:16 MD

Figure 27: Size distributions measured by the CDP, each plot representing 1-s of measurements.



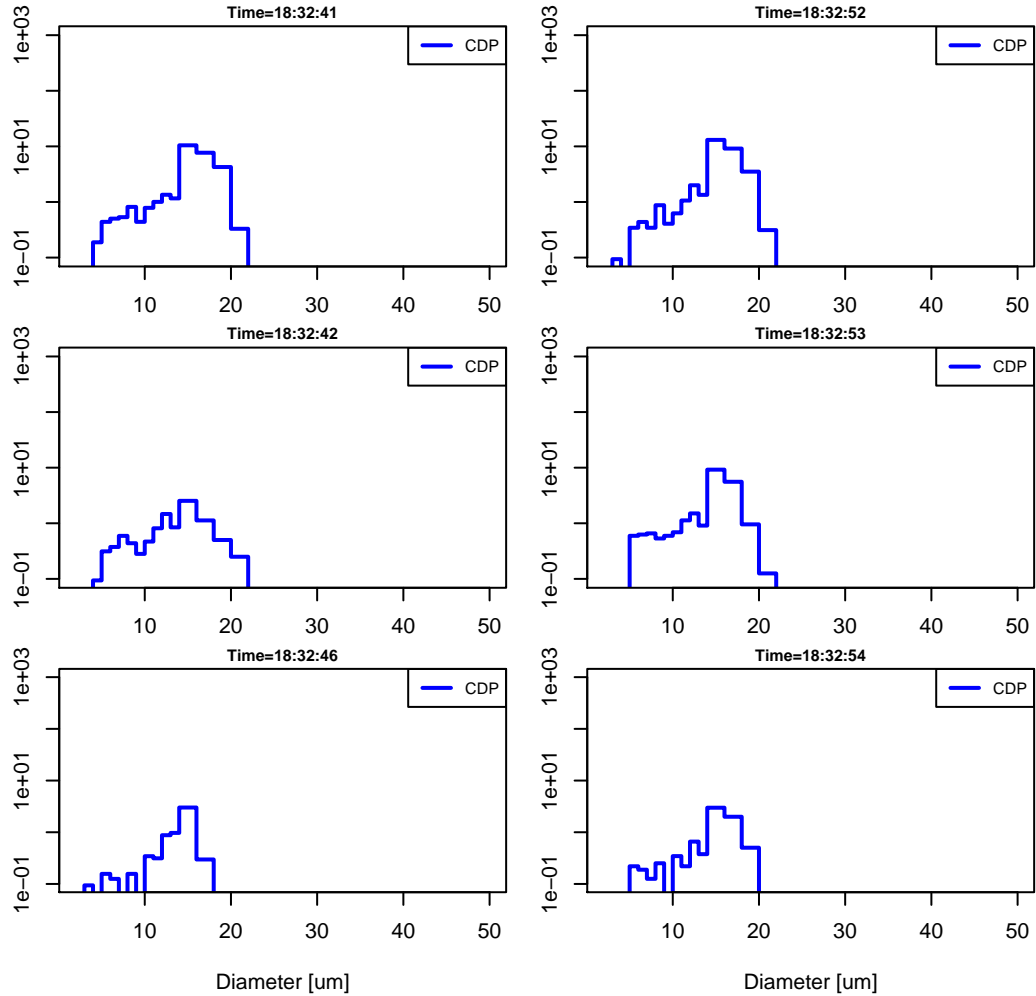
CSET RF03 2015-07-09 14:58:59–23:48:53 UTC, generated by RPlot20 2015-07-14 07:46:16 MD

Figure 28: Size distributions measured by the CDP, each plot representing 1-s of measurements.



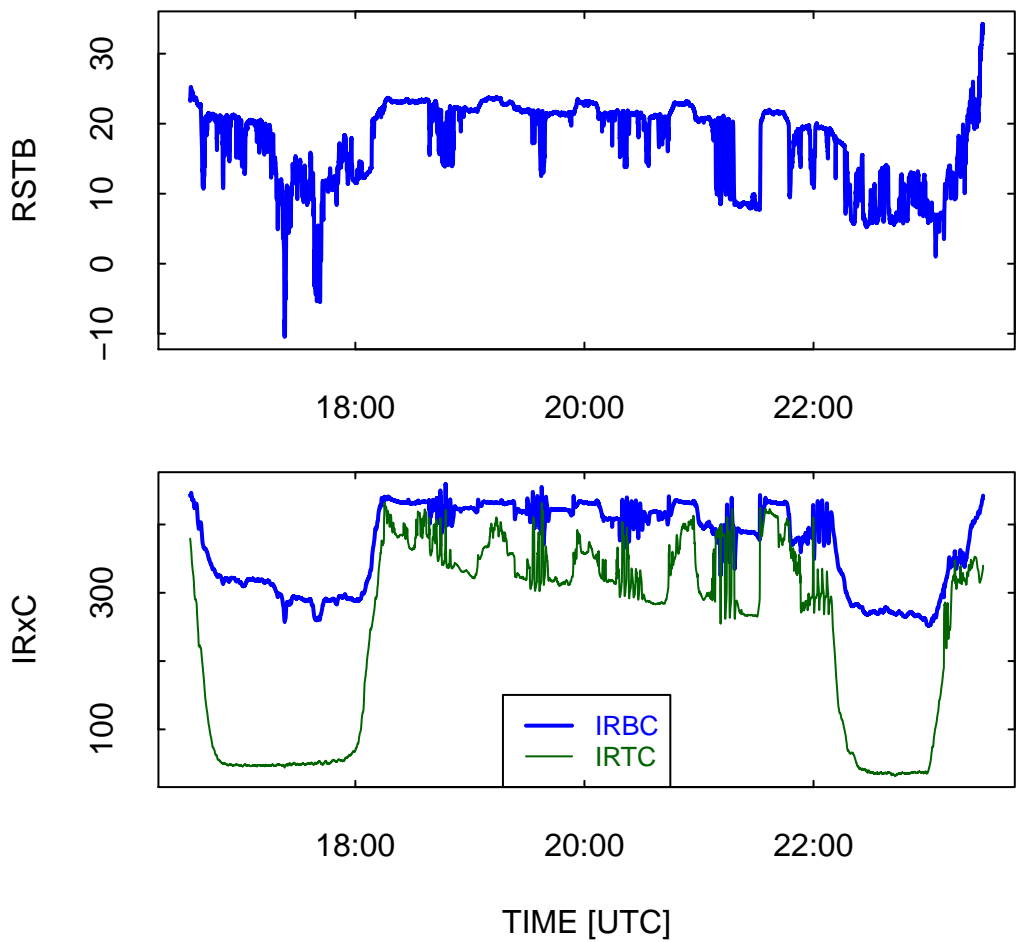
CSET RF03 2015-07-09 14:58:59–23:48:53 UTC, generated by RPlot20 2015-07-14 07:46:16 MD

Figure 29: Size distributions measured by the CDP, each plot representing 1-s of measurements.



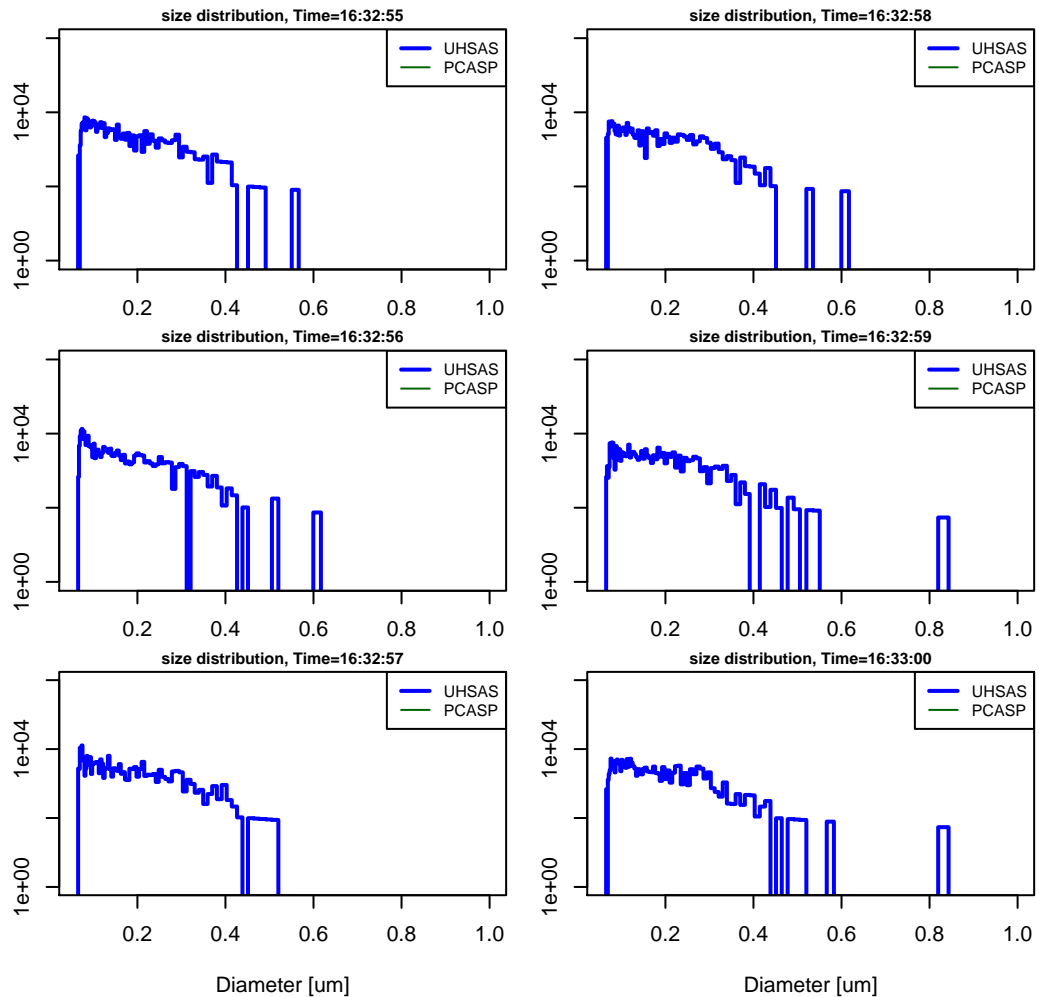
CSET RF03 2015-07-09 14:58:59–23:48:53 UTC, generated by RPlot20 2015-07-14 07:46:16 MD

Figure 30: Size distributions measured by the CDP, each plot representing 1-s of measurements.



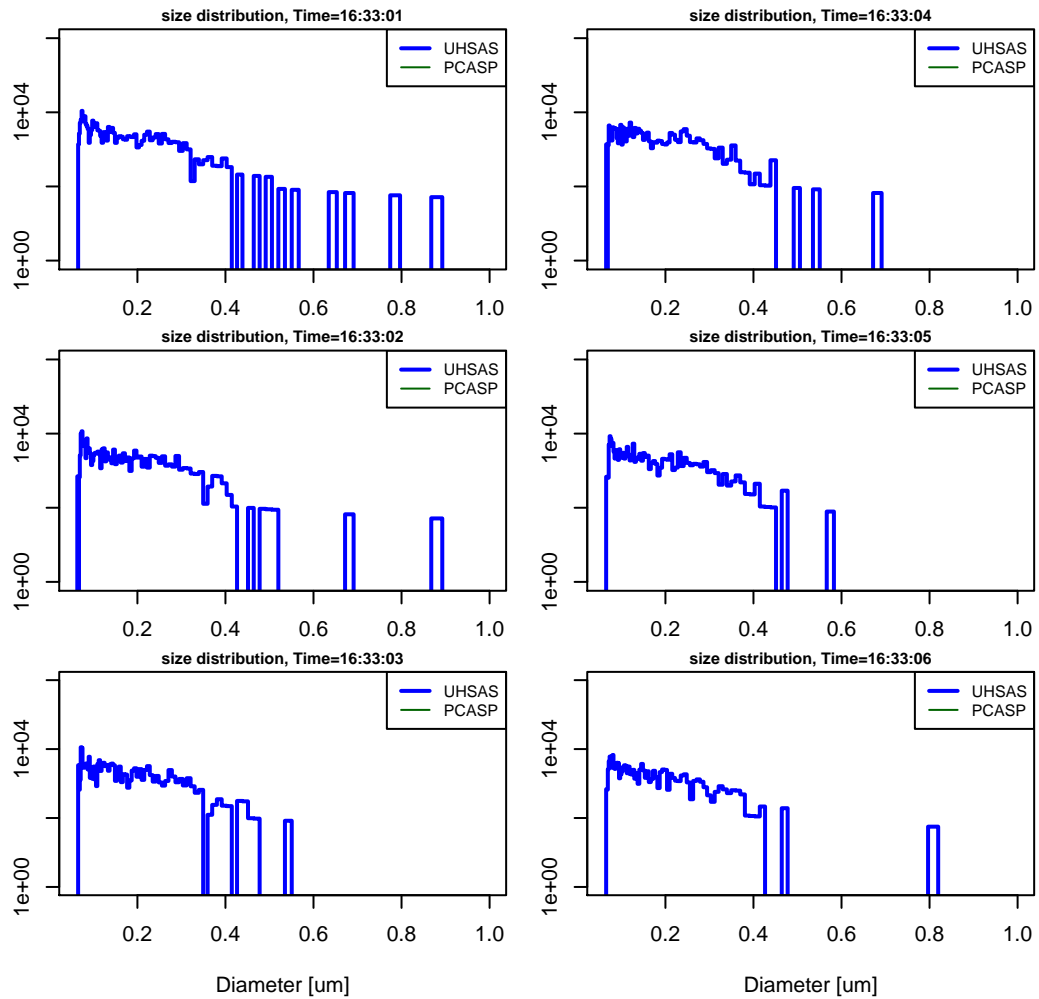
:SET RF03 2015-07-09 14:58:59-23:48:53 UTC, generated by RPlot21 2015-07-14 07:46:16 MD

Figure 31: Surface temperature measured radiometrically (RSTB) [deg.C] (top panel) and infrared irradiance measured by the down-looking (IRBC) and upward-looking (IRTC) radiometers [W/m²]



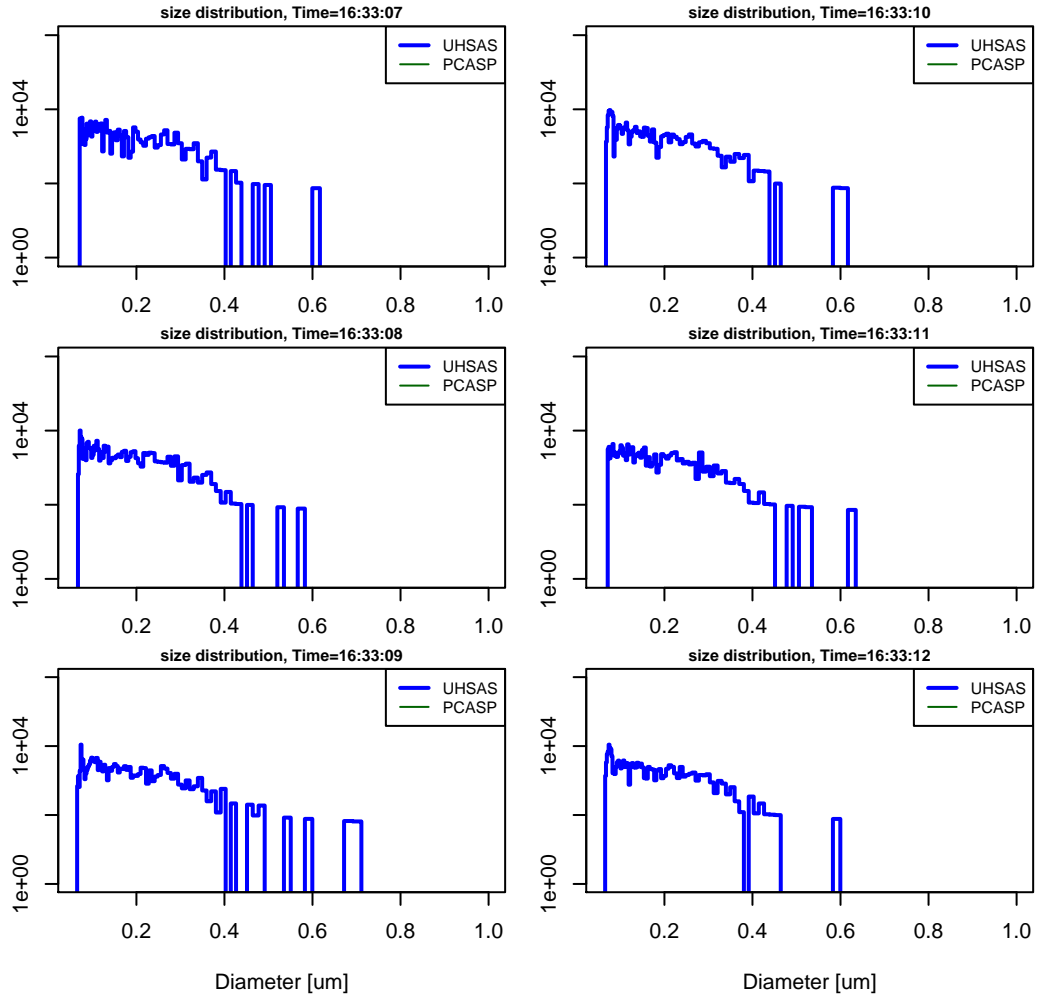
CSET RF03 2015-07-09 14:58:59-23:48:53 UTC, generated by RPlot22 2015-07-14 07:46:16 MD

Figure 32: Size distributions measured by the UHSAS, each plot representing 1-s of measurements.



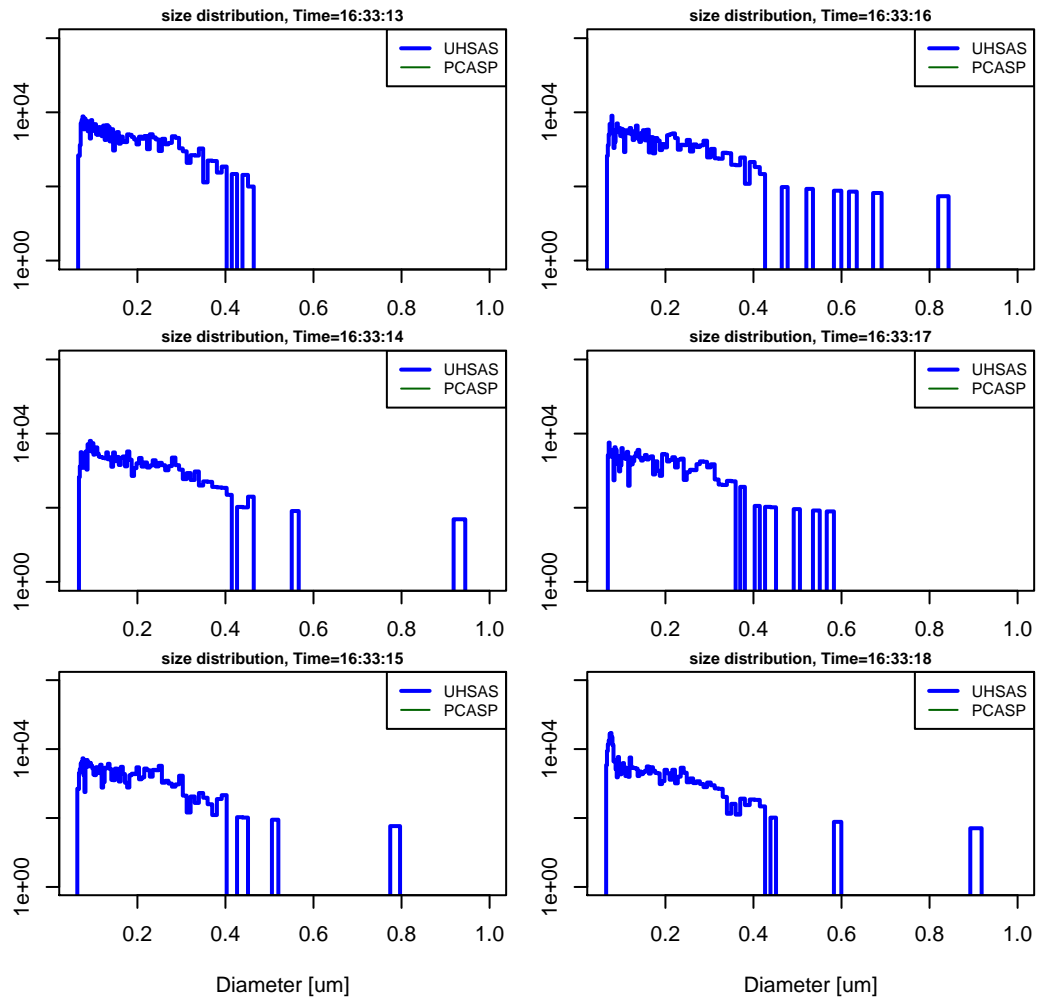
CSET RF03 2015-07-09 14:58:59-23:48:53 UTC, generated by RPlot22 2015-07-14 07:46:16 MD

Figure 33: Size distributions measured by the UHSAS, each plot representing 1-s of measurements.



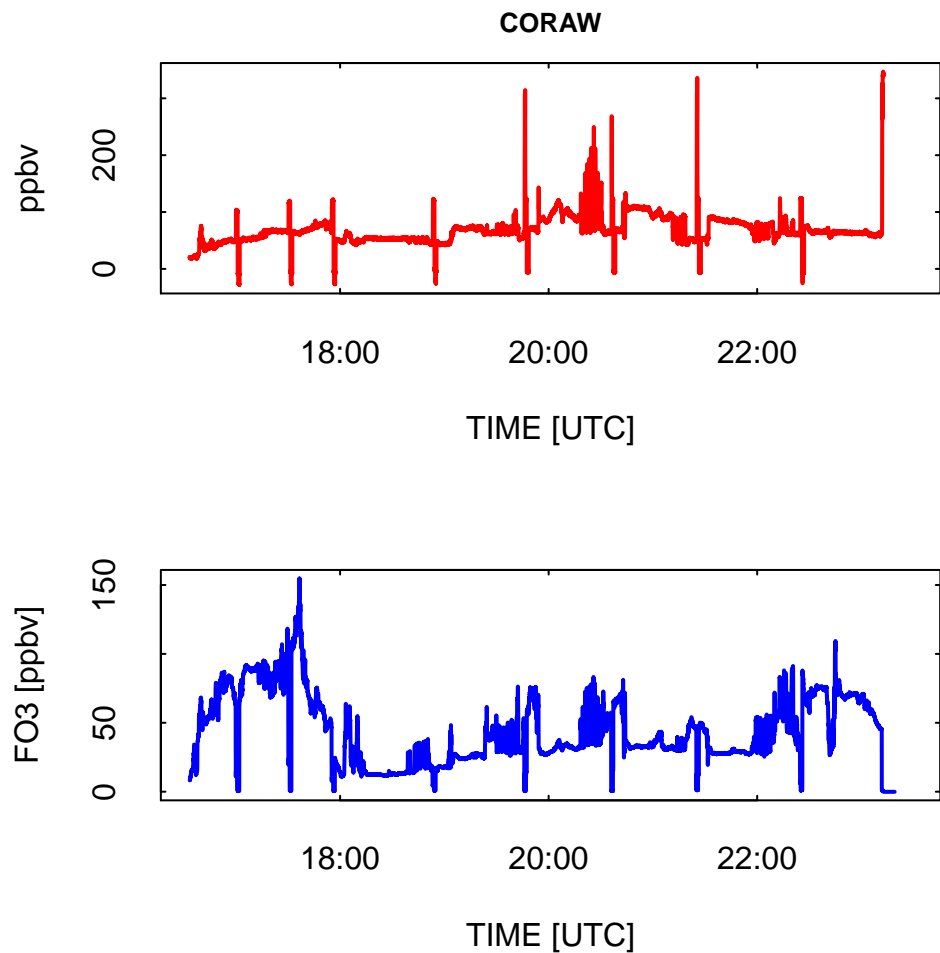
CSET RF03 2015-07-09 14:58:59-23:48:53 UTC, generated by RPlot22 2015-07-14 07:46:16 MD

Figure 34: Size distributions measured by the UHSAS, each plot representing 1-s of measurements.



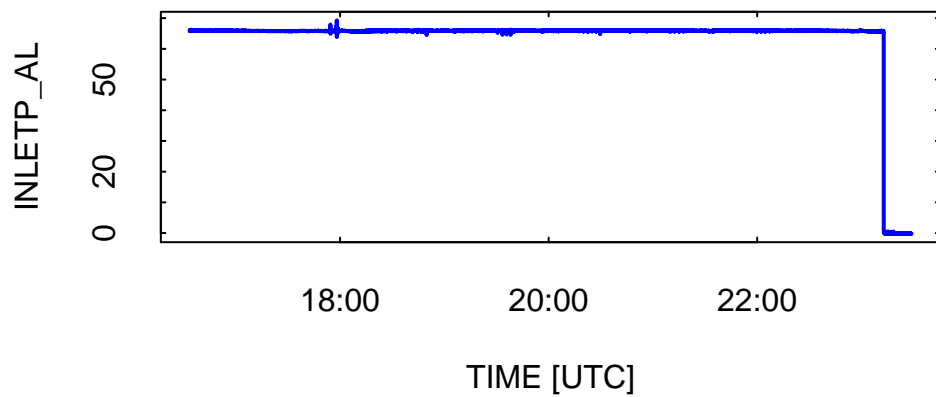
CSET RF03 2015-07-09 14:58:59-23:48:53 UTC, generated by RPlot22 2015-07-14 07:46:16 MD

Figure 35: Size distributions measured by the UHSAS, each plot representing 1-s of measurements.



:SET RF03 2015-07-09 14:58:59-23:48:53 UTC, generated by RPlot30 2015-07-14 07:46:16 MD

Figure 36: Uncorrected CO concentration CORAW and ozone concentration FO3.



:SET RF03 2015-07-09 14:58:59-23:48:53 UTC, generated by RPlot30 2015-07-14 07:46:16 MD

Figure 37: Inlet pressure of the Aerolaser CO instrument, and the flow through that instrument (here missing because there were no valid values for this variable).

Search for maneuvers At the end of the Review.R script there are code segments that do simple searches for candidate time for various maneuvers, including circles, speed runs, pitch maneuvers, yaw maneuvers, and reverse-heading maneuvers. These may be useful when compiling lists of maneuvers for the project. There were no candidates identified for this flight.

4 How to add new plots

Here is the procedure for adding a plot to this routine:

1. Copy this code and insert it in the PlotFunctions directory with a name like RPlot31.R:

```
### This is a model for adding a function:
RPlotN <- function(data) {
  # next just resets geometry, in case previous plot used multiple panes
  op <- par (mfrow=c(1,1), mar=c(5,5,2,2)+0.1)
  ## simplest plot: variables "Var1" and "Var2" vs time
  plotWAC (data[, c("Time", "Var1", "Var2")], ylab="Var")
}
```

2. Change N in the name RPlotN to some number not in use. The present version uses 1–22 and 30, so a good choice might be to use 31; i.e., RPlotN should be replaced by RPlot31.
3. Make sure that any needed variables are in “VarList”. If not, add them in the statement where VarList is defined, or alternately follow that statement (immediately below) with this statement: VarList <- c(VarList, "Var1", "Var2") where Var1 and Var2 are replaced by the names of variables you want to use. They must be in the netCDF file or else this program will stop; it is not protected against this error.
4. Then, follow where the above function definition is inserted with this R code:

```
if (testPlot(31)) {
  source ("PlotFunctions/RPlot31.R")
  RPlot31 (DataV)  # change '31' to whatever number you have used
}
```

5. You can then make additional modifications to the function as you see the results and want to change them. Use the functions RPlot[1:22] in Review.R for ideas of ways to tailor the plots. Also, there are some functions available that you may find useful:

- (a) hline (X) will draw a black dashed horizontal line on the plot at ordinate value X.
 - (b) SmoothInterp (X) will return a smoothed version of X (which might be a variable like data\$TASX) as referenced in your routine). Usage: Xsmoothed <- SmoothInterp (X).
6. Finally, please write a description of how to interpret the new plot and what to look for when reviewing data. Give that to me for incorporation into future versions of this memo.

– End of Memo –

Reproducibility:

PROJECT: CSET
PROGRAMS: Review.Rnw, Review.R
ORIGINAL DATA: /scr/raf_data/CSET/CSETrf03.nc – for testing
GIT: <https://github.com/WilliamCooper/CSET.git>